INVESTIGATING THE USE OF ION EXCHANGE RESINS

FOR PROCESSING BIODIESEL FEEDSTOCKS

A Dissertation

by

YOUSUF JAMAL

Submitted to the Office of Graduate Studies of
Texas A&M University
in partial fulfillment of the requirements for the degree of

DOCTOR OF PHILOSOPHY

Approved by:

Chair of Committee,	Bryan Boulanger
Committee Members,	Bill Batchelor
	Sergio Capareda
	Joshua Yuan
Head of Department,	John Niedzwecki

December 2012

Major Subject: Civil Engineering

ABSTRACT

Ion exchange resins, commonly used in water treatment, demonstrate promise for the production of biodiesel from biomass feedstocks. The goal of this presented PhD research is to investigate novel uses of ion exchange resins for processing biodiesel feedstocks. Specifically, this research explored using ion exchange resins to remove free fatty acids (FFA) from soybean and waste cooking oils, catalyze transesterification of soybean oil, and catalyze in-situ conversion of dried algal biomass to biodiesel and other recoverable organics.

The effect of temperature, moisture content, mixing rate, and resin drying on deacidification of soybean oil with 5% oleic acid feedstock was explored using Dowex Monosphere MR-450 UPW within a batch reactor. The resins were observed to remove up to 83 ± 1.3% of FFA from soybean oil with less than 5% moisture content while operated at a 20% resin loading at 50 °C while mixing at 550 rpm. Once operation characteristics impacting deacidification were evaluated, a series of experiments were carried out to demonstrate the use of mixed bed resin to remove FFA from waste cooking oils. An investigation of wash solutions capable of regenerating the resins was also carried out. Using methanol to regenerate the resins resulted in more than 40% FFA removal over three regeneration cycles, highlighting the utility of resin regeneration as a cost saving measure.

Transesterification of soybean oil on Amberlyst A26-OH, a basic ion exchange resin, in the presence of excess methanol was carried out to determine the mechanism of the

reaction occurring on the surface. A batch reactor approach was used and reactions were carried out with and without FFA present in the soybean oil feed stock at a 20% resin loading at 50 °C while mixing at 550 rpm. When FFA was present in the feedstock and methanol is present in excess, the rate constant for methanol consumption increased. Based upon model fitting, the rate constant of methanol consumption was determined to be 2.08×10^{-7}/sec with FFA absent and 5.39×10^{-4}/sec when FFA is present when the Eley-Rideal model was used to fit the data.

In-situ conversion of dried algal biomass to biodiesel and other recoverable organics was investigated using a batch reaction system with 1 gram of algae. The system was operated with 40:60 methanol:hexane as the solvent system operated at 50 °C while mixing at 550 rpm over a range of catalyst loadings. The highest observed ester yield, approximately 60% yield (37 mg_{ester}/g_{algae}), was observed when air dried algae was reacted with a 20% resin. An evaluation of the reaction products showed a mixture of esters, phytol, alcohols, and ketones; highlighting the complexity of the reactions occurring during in-situ biomass conversion.

DEDICATION

This research is dedicated to my family, friends, and teachers who have shown their confidence and support towards my success.

“Only one who devotes himself to a cause with his whole strength and soul can be a true master. For this reason mastery demands all of a person.” - Albert Einstein

ACKNOWLEDGEMENTS

I wish to acknowledge my adviser Dr. Bryan Boulanger for giving me the chance to learn and achieve my research goals while supporting me emotionally and by providing motivation whenever required. I would also like to thank my committee members, Dr. Bill Batchelor, Dr. Sergio Capareda and Dr. Joshua Yuan, for sharing their knowledge and guidance. I also wish to thank the Fulbright organization for funding my PhD research stipend, supporting my travel costs, and contributing to a portion of the laboratory analytical costs. I am also grateful to AlgEternal Technologies, LLC for supplying the algae used in my research. GC-MS analysis was conducted on a fee-per-use basis by Dr. Yohannes H. Rezenom in TAMUs Department of Chemistry. Along the way the laboratory portions of the research were also aided by Manasi Mahish, Rachel Thompson, Guofan Lao and Charlie Kuo (all current or former laboratory group members); many thanks to each of them.

Modeling discussions also occurred between Ahmed Rabia (a PhD Candidate of the Petroleum Engineering Program at TAMU) and Dr. Benjamin Wilhite from TAMUs Department of Chemical Engineering. I am also very grateful to Rhykka Connelly, the technical director of the University of Texas Algae Science and Technology Facility, who proved invaluable at helping with the lipid analysis of the algae samples. Finally and most importantly, I thank my parents, wife, and loved ones for their prayers, encouragement, and patience as I make my journey towards knowledge.

NOMENCLATURE

AOCS	American Oil Chemists' Society
ASTM	American Society of Testing Materials
DIN	German Institute for Standardization (English)
EN	European standard
FAME	Fatty Acid Methyl Esters
FFA	Free Fatty Acid
MeOH	Methanol
Stdev	Standard deviation
TAMU	Texas A&M University
GC-MS	Gas Chromatography-Mass Spectrometer
PhD	Doctor of Philosophy
°C	Degrees Centigrade
C_n	Carbon chain length with *n* units
US	United States
R	any long chain alkyl group
R'	any alkyl group of length C_1-C_4
ER	Eley-Rideal
LHHW	Langmuir-Hinshelwood-Hougen-Watson
HPLC	High Performance Liquid Chromatography
H_2SO_4	sulfuric acid
NaOH	sodium hydroxide

WCO	Waste Cooking Oil
rpm	rotations per minute
mL	milliliter
g	gram
mg	milligram
ANOVA	Analysis of Variance
S-DVB	styrene-divinylbenzene
H^+	hydrogen
OH^-	hydroxide
eq	equivalence
L	Liter
kg	kilogram
ft^3	cubic foot
$CaCO_3$	calcium carbonate
µm	micrometer
min	minimum
%	percent
p	p-value
µL	microliter
ID	Inner Diameter
Δq	root mean square error
r^2	linear correlation coefficient

$[E]_t$	concentration of esters at any time *t*
n	number of replicates
mm	millimeter
hr(s)	hour(s)
A_{ISD}	peak area of the internal standard
G_C	Group content
$\sum A$	total area
C_{ISD}	Concentration of internal standard
V_{ISD}	Volume of internal standard
m	weighed mass of analyzed sample
Keq	methanol equilibrium constant for adsorption
K_A	equilibrium adsorption constant for diglyceride, monoglyceride, glycerol and esters
MeOH*	methanol on the catalyst surface
T	triglyceride
T*	triglyceride on the catalyst surface
E	ester
E*	ester on the catalyst surface
D*	diglycerides on the catalyst surface
FFA*	free fatty acid on the catalyst surface
M*	monoglycerides on the catalyst surface
k_x	reaction rate constant where *x* ranges from 1 to 7
k_n	generic forward reaction rate, *n*

k_{-n}	generic reverse reaction rate, *-n*
D	diglycerides
M	monoglycerides
G	glycerol
G*	glycerol on the surface of the catalyst
*	resin surface
S_T	total binding sites on resin surface
n	reaction step
$k_{adsorption}$	adsorption rate constant
$k_{desorption}$	desorption rate constant
K_x	equilibrium rate constant where *x* varies from 1 to 7
r_1	rate of methanol consumption
MALDI	Matrix Assisted Laser Desorption/Ionization
TOF	Time of Flight

TABLE OF CONTENTS

Page

Page

Page

LIST OF FIGURES

Page

Page

LIST OF TABLES

Page

1. INTRODUCTION

Biodiesel is a transesterified or esterified alkyl ester product of lipid based feedstocks. Biodiesel production has received attention during the last few decades due to the fuel's low sulfur and carbon dioxide emissions[1], environmental biodegradability[2], and the use of variable feedstocks for biodiesel production[3-7]. Conventionally, biodiesel is produced through a multiple unit process system involving chemical or mechanical extraction of lipids from plant or animal derived feedstocks. As shown in Figure 1.1, the extracted lipids are then reacted with a homogeneous catalyst (sodium or potassium hydroxide) in the presence of C_1-C_4 alcohols (methanol, ethanol, or butanol) to produce alkyl esters through transesterification at operating temperatures ranging between 60 and 100 °C.

Depending upon the composition of the extracted lipids (triglycerides, diglycerides, monoglycerides, phospholipids, sterols, glycolipids, and free fatty acids) additional purification of either the feedstock or the reaction products may be required to increase biodiesel yield[8-10] and meet ASTM standard D 6751 or European standard DIN EN 14214 requirements for biodiesel composition[11-12]. As of July 2012 there are 195 biodiesel plants operating in the US with a production capacity approaching 2.9 billion gallons per year [13]. Thirteen new plants are currently under construction[14] and once they are brought online they will increase the US production

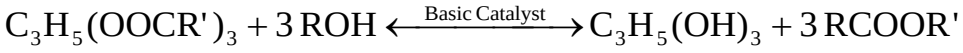

Figure 1.1 Transesterification reaction where R' could be any long chain alkyl group and R any alkyl group of length C_1-C_4.

capacity by an additional 400 million gallons.

However, according to the US Department of Energy the current rate of US biodiesel production from vegetable oil based feedstocks is only 0.58% of the overall diesel demand. To realize a higher fraction of total demand met by biodiesel without sacrificing the environment or food sources, wastes feedstocks must be utilized. Wastes feedstocks that should be considered include waste greases[15], waste cooking oils[16], wastewater sludges[17-18] and algal biomass[19]. All of these alternatives are a cheap source of lipids for biodiesel production. However, they also each pose challenges to current processing methods[18].

While transesterification is a simple and well understood reaction process, the presence of any impurities in biodiesel feedstocks cause problems during conventional homogeneous catalyst based processing and require further unit processing to achieve the same biodiesel product quality. The two impurities presenting the greatest challenge to conventional processing methods include feedstock moisture and free fatty acid contents. Presence of water in feedstocks leads to hydrolysis of triglycerides[20] and results in the formation of free fatty acids (FFA), diglycerides, monoglycerides and glycerin. The presence of FFA in feedstocks processed with homogenous catalysts leads to saponification resulting in poor separation of reaction products[20- 21].

Deacidification (removal of FFA) is accomplished in conventional biodiesel processing by reacting FFA containing triglyceride feedstock with a homogeneous acid catalyst (including sulfuric or hydrochloric acids). Deacidification is desirable in feedstocks having greater than 1% FFA content by weight[22]. Acid catalysis converts

FFA in the feedstock into esters through the process of esterification shown in Figure 1.2[23]. Esterification of FFA rich feedstocks with homogeneous acidic catalysts slow down the ester formation process, because water formed during the reaction poisons the catalyst and reduces alkyl ester yield[23]. Homogeneous catalysts are also consumed through reaction of FFA in the feedstock resulting in increased production costs. Therefore, alternative deacidification processes are of broad interest; especially for feedstocks with high FFA and/or water content.

Alternative deacidification processes reported in the literature include the use of enzymes[24], catalytic and non catalytic supercritical reaction conditions[25-26], solvent extraction[27], and ion exchange resins. Ion exchange based deacidification processes have become a preferred alternative, because ion exchange systems are easier and more cost efficient to run compared to enzymatic, supercritical, and solvent based systems. They can also be run at low temperature (less than 60 °C) and ambient pressure operating conditions, making ion exchange based processing options safer and more desirable for scale up. Ion exchange resin based processing systems also offer an economic advantage of the other alternatives due to the fact that they may be recovered and regenerated[28]. Because they were designed for use in aqueous systems, ion exchange resins also offer the advantage of maintaining their performance in the presence of moisture (water) and also possess capacity to sorb water in high oil content systems.

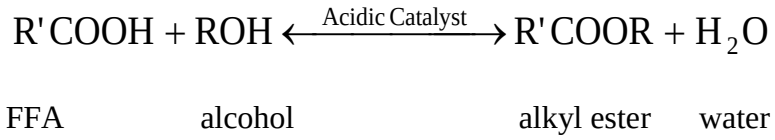

Figure 1.2 Esterification reaction where R' could be any long chain alkyl group and R any alkyl group of length C_1-C_4.

Ion exchange resins are documented to remove FFA from the triglyceride feedstocks either through adsorption of FFA onto the surface of the basic ion exchange resins or through reactivity with functional groups present on the surface of acidic ion exchange resin[29]. Acidic ion exchange resins also may be used effectively as heterogeneous catalysts to convert FFA within oil feedstocks into alkyl esters[30] through esterification (Figure 1.2). However, a long reaction time is required to complete deacidification and esterification. Basic ion exchange resins also serve as heterogeneous catalysts to foster transesterification (Figure 1.1) at the site of the surface bound functional groups in the presence of alcohol[31]. Use of basic ion exchange resins also has the potential for reducing the FFA content of feedstocks through adsorption of the negatively charged FFA to the positively charged basic site on the resin[20, 32].

Because alternative feedstocks contain higher amounts of residual impurities, processing alternative feedstocks into biodiesel requires modification to existing production processes. Ion exchange resins offer unique abilities to handle impurities while deacidifying or catalyzing reactions. Therefore, investigating the use of ion exchange resins to deacidify and facilitate transesterification processes in these alternative feeds is essential to expanding biodiesel production.

Another advancement that will expand biodiesel production capacity is the development of in-situ processing (simultaneous extraction and conversion) techniques. In-situ processing will further limit the number of unit processes and reduce production costs associated with processing conventional and alternative biodiesel feedstocks. Initial investigations indicate in-situ processing will reduce processing time and cost

while demonstrating reasonable reaction yield[33]. The same co-solvent mixtures used in conventional processing are also used in in-situ processing; however, the homogeneous catalyst and alcohol are added simultaneously[34]. Because homogeneous catalysts are consumed, the use of heterogeneous catalysts within in-situ reaction systems is of interest.

Reports on the in-situ transesterification or esterification of extracted oil lipids using heterogeneous basic and acid catalysts are being to appear in the literature[35-38]. These existing reports focus predominantly on the use of alumina and metal oxide based catalysts to foster transesterification and use of sulfonic acid within an organic support to facilitate the reactions (esterification). Additionally, to the best of our knowledge, only a single report explores the use of heterogeneous catalysts for in-situ processing of algae biomass. In their study Li *et al.*[39] report on the use of in-situ heterogeneous transesterification of algae using an amended soxhlet extractor with a methanol-dichloromethane co-solvent system in the presence of a magnesium-zirconium basic solid catalyst. However, the amended soxhlet system was not true in-situ processing, as the solvent was recirculated through the algae biomass while the transesterification reactions occurred in a separate vessel in the Soxhlet system.

Another area of advancement within alternative biodiesel feedstock processing is the realization of additional recoverable organics during biodiesel production. Current investigations on the use of ion exchange resins have solely focused on the biodiesel yield, but have not focused on the yield of other recoverable organics present in the complex reaction mixture. Other biomolecules of interest that are potentially formed

and recoverable during the extraction and conversion of feedstocks using heterogeneous catalysts include aldehydes, alcohols, alkanes, glycerol, and glycerol byproducts.

Examples of potential reactions of glycerol during processing can be inferred from the literature (glycerol reaction in other systems) and include hydrogenolysis of glycerol to propylene glycol[40]; dehydration of glycerol to acrolin in the presence of an acidic catalyst[41]; and etherification of glycerol in the presence of hydrocarbons resulting in tertiary ethers[42]. The use of ion exchange resins as catalysts to facilitate additional reactions aimed at recovering value added organics during processing of alternative feedstocks would be an exciting realization. However, these reaction products have not been previously examined in heterogeneous catalysts systems used for processing biodiesel largely because other researchers do not appear to have looked for them.

The field of biodiesel research and production has increased exponentially in the past two decades. However, additional processing options must be realized if biodiesel will be adopted at a larger market share within the existing US economy. Alternative feedstocks must also be examined for their ability to produce biodiesel and additional recoverable organics. Use of ion exchange resins under low temperature and pressure processing conditions offer distinct advantages to conventional processing methods. However, challenges remain to their use for deacidification and in-situ transesterification/conversion of biodiesel feedstocks. This research addresses several of the challenges identified in this introductory section by investigating novel uses of ion exchange resins for biodiesel feedstock processing.

2. PROJECT GOAL AND OBJECTIVES

The goal of this proposed research was to investigate novel uses of ion exchange resins for processing biodiesel feedstocks. To meet the stated goal, three primary objectives were established and investigated. The three objectives were:

Objective 1: evaluate the use of Dowex Monosphere MR-450 UPW resin to deacidify high free fatty acid feedstocks;

Objective 2: model transesterification of soybean oil feedstocks when Amberlyst A26-OH is used as a catalyst; and

Objective 3: explore in-situ conversion of dried algal biomass to biodiesel and other recoverable organics using Dowex Monosphere MR-450 UPW and a mixture of Amberlyst A26-OH and Dowex Monosphere M31 resins as catalysts.

Objective 1 research evaluated deacidification of a 5% oleic acid in soybean oil feedstock to determine the impact of reaction parameters on initial reaction kinetics for the sorption of FFA onto Dowex Monosphere MR-450 UPW (a mixed bed ion exchange resin). The *primary hypothesis* explored within Objective 1 research is that *deacidification using ion exchange resins is impacted by operational parameters including temperature, moisture content, mixing rate, and resin preparation.* Therefore, the effect of temperature, moisture content, mixing rate, and resin drying on resin

performance was explored under laboratory controlled conditions. Following the exploration of the impact of operational characteristics on deacidification, a series of resin regeneration experiments were conducted in order to determine wash solution formulations with potential to regenerate the resin. Finally, a series of experiments were carried out to demonstrate the use of mixed bed resins to remove FFA from waste cooking oils. The experimental methods and results from Objective 2 research are found in Section 3.

Objective 2 research evaluated the potential for Amberlyst A26-OH (a basic ion exchange resin) to be used for transesterification of soybean oil and 5% oleic acid in soybean oil feedstocks. The evaluated process involved adding methanol to the feedstocks in the presence of the ion exchange resin operated at 50 °C and under atmospheric pressure. The *primary hypothesis* explored in Objective 2 research is that *when methanol is in excess the presence of FFA decreases the rate constant for methanol consumption.*

Two kinetic models, Eley-Rideal (ER) and the Langmuir-Hinshelwood-Hougen-Watson (LHHW), were used to evaluate methanol consumption during the reaction. The ER model assumes that transesterification occurs between adsorbed methanol and triglycerides in bulk solution and LHHW model assumes that the surface reaction occurs with both methanol and triglycerides adsorbed to the resin. Additional modifications are made to each model to account for the presence of FFA in solution, as FFA also sorbed to the surface of the resin. The adsorbed FFA blocks reaction sites, but does not take

part in transesterification. The experimental methods and results from Objective 2 research are found in Section 4.

Objective 3 research explored in-situ conversion of algae biomass using a hexane/methanol co-solvent extraction system with heterogeneous mixed bed ion exchange resins. The *primary hypothesis* explored in Objective 3 research is that *simultaneous extraction and conversion of algae to recoverable organics can be achieved in a methanol:hexane solvent system with mixed bed ion exchange resins present as catalysts.* A batch reactor design was used to assess the time series in-situ conversion of algae to recoverable organics at 50 °C and under atmospheric pressure given various processing conditions. Gas chromatography-mass spectrometry (GC-MS) analysis of the time series reaction products was evaluated to identify extraction and conversion products that occurred in the system. The system was evaluated to determine whether in-situ transesterification was observed and whether produced esters underwent additional reactions to form secondary products. Production of other biomolecules was also evaluated through reaction product evaluation with GC-MS. The experimental methods and results from Objective 3 research are found in Section 5.

3. EVALUATING THE USE OF DOWEX MONOSPHERE MR-450 UPW TO DEACIDIFY HIGH FFA FEEDSTOCKS (OBJECTIVE 1)

Objective 1 Hypothesis: Deacidification using ion exchange resins is impacted by operational parameters including temperature, moisture content, mixing rate, and resin preparation.

3.1 Experimental Methods

3.1.1. Materials and reagents Dowex Monosphere MR-450 UPW, 90% commercial grade oleic acid, and degummed soybean oil were purchased from Sigma-Aldrich (St. Louis, MO). Phenolphthalein and potassium hydroxide were purchased from Fisher Scientific (Pittsburgh, PA). Reagent grade toluene, HPLC grade methanol (MeOH), HPLC grade isopropyl alcohol, sulfuric acid (H_2SO_4), sodium hydroxide (NaOH), and citric acid were purchased from VWR International (Sugarland, TX). A feedstock consisting of 5% oleic acid in degummed soybean oil (mass:mass) was prepared fresh daily and used in experiments. WCO was collected from two local food service facilities.

3.1.2. Experimental setup All feedstocks used in the experiments were analyzed for initial FFA content following the American Oil Chemist Society Method Cd 3a-63(1989) prior to use. The reactor system (shown in Figure 3.1) consisted of triplicate 1 L three neck flat bottom flasks containing 200 g of feedstock. A stir bar was added to

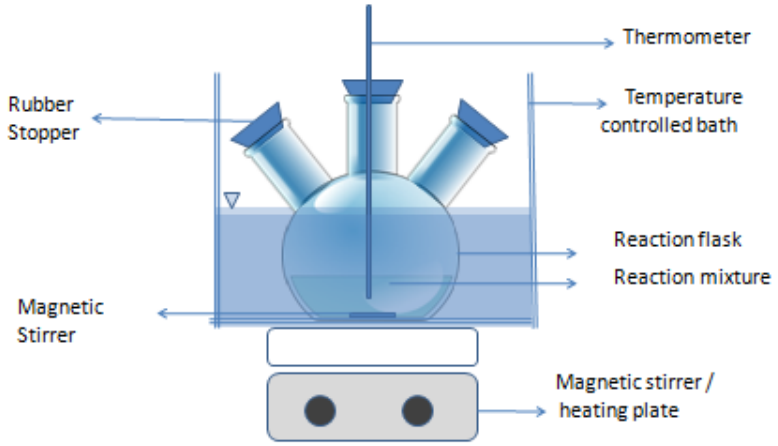

Figure 3.1 Batch reactor setup for deacidification reactions.

each flask and each flask was placed into a water bath sitting on a combination stirring/heating plate. A thermometer was used to measure temperature within the reactor. Reactor necks were sealed during the experiments. All experiments started by reacting 200 g of the feedstock oil with a 20% resin loading (mass:mass). The resin used in each experiment was either fresh resin as supplied (used to determine the effect of temperature, feedstock moisture content, and mixing rate) or solvent washed resin (used to evaluate the effect of wash solvents on resin regeneration).

3.1.3. Deacidification of laboratory prepared 5% oleic acid in soybean oil using Dowex Monosphere MR-450 UPW 200 g of laboratory prepared feedstock were mixed with Dowex Monosphere MR-450 UPW resin at a resin loading of 10% and 20%. Deacidification of the feedstock as a function of time was measured at a reaction temperature of 50 °C and a mixing rate of 550 rpm. FFA levels in the mixing vessel were measured at 0, 2, 4, 6, and 8 hours following the American Oil Chemist Society Method Cd 3a-63(1989). Triplicate evaluations for each resin loading were used to examine deacidification using the resin.

3.1.4. Effect of temperature, feedstock moisture content, and mixing rate on FFA removal Factors affecting feedstock deacidification were studied using the laboratory prepared 5% oleic acid in soybean oil feedstock. During the experiments the reaction temperature, feedstock moisture content, and the reactor mixing rate were varied to determine their effect on deacidification of the feedstock using the mixed bed resin. The temperature effect on FFA removal was evaluated at 25, 35, and 50 °C by controlling the temperature of the water bath. The effect of feedstock moisture content on FFA removal

was evaluated for feedstock moisture contents of 0, 2.5, 5.0, 7.5, and 10 percent moisture. Moisture was added to the initially prepared 5% oleic acid soybean oil mixture by adding a specified amount of water to the mixture based on the desired weight percent. The mixing rate effect on FFA removal was evaluated at 0, 125, 250 and 550 rotations per minute (rpm) by adjusting the stirring speed of the stir plate. Following each experiment, 2.5 g samples of the reacted solution were analyzed for FFA content using the American Oil Chemist Society Method Cd 3a-63(1989) to determine the amount of FFA removed due to each experimental condition.

3.1.5. Resin regeneration with solvent washing A series of experiments were carried out on FFA loaded resin to explore the effect of using different wash solvents on resin regeneration and reusability. The wash solvents evaluated in this study included MeOH, 1% and 5% NaOH in MeOH, 5% NaOH in water, a mixture of 5% H_2SO_4/NaOH in MeOH, a mixture of 5% citric acid/NaOH in MeOH, a mixture of hot MeOH with 5% NaOH (25 mL of each solvent in mixture), and hot MeOH only. Hot MeOH was MeOH heated to 50 °C prior to rinsing. Wash experiments were carried out in triplicate by washing a measured amount of reacted resin that was separated from the initial oil step through gravity filtration with 25 mL of each solvent or solvent mixture.

The solvent or solvent mixture was poured over the resin retained on the filter and passed through the resin by gravity flow. Single cycle regeneration experiments were conducted with 200 g of new 5% oleic acid soybean oil, the regenerated resin at a loading rate of 20 ± 1%, a reaction temperature of 50 °C, a feedstock moisture content of less than 1%, and a mixing rate of 550 rpm. The effect of drying the resin following

washing was also evaluated by varying the drying time from 0, 9, and 18 hours. Finally, experiments were carried out using MeOH and 1% NaOH in MeOH over three regeneration cycles to evaluate the suitability of continued regeneration for FFA removal. The FFA content of the oleic acid soybean mixture following reaction with the regenerated resin was measured for each single cycle regeneration experiment and for a three cycle regeneration experiment.

3.1.6. Effect of feedstock on deacidification using heterogeneous resin The effect of different feedstocks with varying levels of FFA content was examined to determine the robustness of application of the Dowex Monosphere MR-450 UPW resin for FFA removal. Feedstocks evaluated in this portion of the study included two waste cooking oils (WCOs) obtained from local sources. The effect of the feedstock was carried out with a resin loading rate of 20 ± 1%, a reaction temperature of 50 °C, a feedstock moisture content of less than 1%, and a mixing rate of 550 rpm. The acid value of the feedstock was measured over a time series to determine the FFA removal over the course of the reaction[43].

3.1.7. Statistical evaluation of the data Data from the experiments were statistically evaluated using SPSS Statistics version 19. Statistical relationships were evaluated using single step analysis of variance (ANOVA) at the 95% confidence interval around the null hypothesis that there are no differences between mean values of FFA removal across experimental treatments. If the null hypothesis was rejected, a follow up post-hoc multiple comparisons test (Tukey's test) was used to determine the statistical relationship within the data.

3.1.8. Properties of mixed bed resin Dowex Monosphere MR-450 UPW is a bi-functional styrene-divinylbenzene (S-DVB) based non-separable, mixed bed, gel-type, ion exchange resin with sulfonic acid (350 UPW) and quaternary ammonium (550 UPW) functionality. S-DVB resins are stable across a range of reaction temperatures and do not degrade easily due to high shear mixing rates[38] . The properties of Dowex Monosphere MR-450 UPW are summarized in Table 3.1.

3.2 Results and Discussion

3.2.1. Deacidification of laboratory prepared 5% oleic acid in soybean oil feedstock using Dowex Monosphere MR-450 UPW resin Figure 3.2 demonstrates deacidification as a function of time using Dowex Monosphere MR-450 UPW. The resin was observed to remove FFA residuals to below 1% within two hours at a mixing rate of 550 rpm, a reaction temperature of 50 °C, and a resin loading of 20%. At a 10% resin loading the FFA residuals in the feedstock only reduced to 2.5% under the same reaction conditions. Because no primary alcohols were added to the system, the observed deacidification is hypothesized to be caused through adsorption of oleic acid to the basic quaternary ammonium site present on the surface of the resin. The difference in FFA removal between the 10% and 20% resin loading provides evidence to support this hypothesis, which is also presented within the literature for basic ion exchange resins in the presence

Table 3.1 Properties of Dowex Monosphere MR-450 UPW[44-45] . (Adapted with permission from The Dow Chemical Company, copyright 2002).

Specifications	Units	H^+ form	OH^- form
Total exchange capacity, minimum	eq/L	1.9	1.0
Total exchange capacity, minimum	kg/ft^3 as $CaCO_3$	41.5	21.9
Water retention capacity	%	46-53%	55-65%
Mean particle size	µm	360±50	590±50
Uniformity coefficient, maximum	µm	1.1	1.1
Whole uncracked beads, minimum	%	95	95
Crush strength	g/bead	350	350
Average, minimum >200	%	95	95
Particle density, approximate	g/mL	1.22	1.08
Cationic resin conversion to H^+, minimum	%	99.7	-
Cationic resin conversion to OH^-, minimum	%	-	95

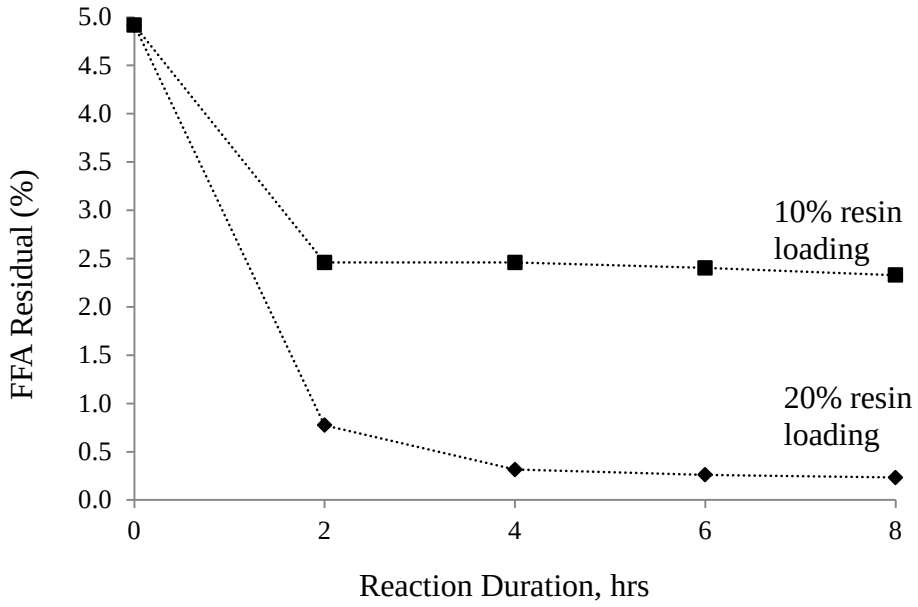

Figure 3.2 Deacidification of 5% oleic acid in soybean oil feedstock by Dowex Monosphere MR-450 UPW.

of primary alcohols[27, 46-47] . Rapid removal of FFA on basic ion-exchange resins in absence of alcohol has also been reported[48] .

3.2.2. Effect of temperature, feedstock moisture content, and mixing rate on FFA removal An increase of reaction temperature was determined to increase deacidification within all reactors during a 2 hour reaction duration, a constant mixing rate of 550 rpm, and an initial FFA content of 5%. FFA removal ranged from a low of 20 ± 5.3% FFA removal at 25 °C up to 79 ± 1.3% FFA removal at 50 °C. The mean FFA removal observed as a function of temperature was not statistically similar ($p<0.05$) and follow up multiple comparison testing indicated that the observed mean %FFA removal increased with corresponding increases in temperature. According to the resin characteristics provided by Dow, Dowex Monosphere MR 450 UPW resins have a maximum operating temperature of 60 °C. Previous attempts to run the reaction at 60 °C or above resulted in loss of performance and 50 °C was set at the maximum test point in this study. The effect of temperature on heterogeneous resin processing of feedstocks has been previously demonstrated for esterification of waste fried oil[30, 49] , but not for feedstock deacidification using mixed bed resin.

The mean %FFA removal due to increases in feedstock moisture content was also found to not be statistically similar across a range of moisture contents ($p<0.05$). Follow up multiple comparisons testing revealed that an increase of feedstock moisture content was observed to decrease mean %FFA removal at feedstock moisture contents above 5% at 550 rpm mixing rate and a reaction temperature of 50 °C. Below 5% feedstock

moisture content, mean FFA removal from the feedstock averaged 87 ± 3.9% with mean FFA removal for 0, 2.5 and 5% moisture contents being statistically similar ($p>0.05$). Above 5% moisture content the mean FFA removal due to reactivity with the resin decreased from 83 ± 1.3% at 5% moisture content down to 71 ± 3.9% and 55 ± 1.3% for 7.5% and 10% moisture content, respectively. Mean FFA removal observed for 7.5 and 10% feedstock moisture contents were not statistically similar in comparison to each other ($p<0.05$) or to FFA removal observed for 0, 2.5, and 5% moisture contents ($p<0.05$).

System performance indicates that feedstock moisture contents below 5% do not interfere with FFA removal using the resin; therefore, remaining experiments were carried out with feedstocks received as provided from the vendor. Additionally, because MeOH was not added to the system, formation of water during the deacidification reaction is not expected [30]. The resulting decrease in FFA removal observed due to the presence of water is proposed to be caused by formation of a hydration layer near the resin's functional sites that interferes with FFA adsorption[1].

The mixing rate in the reactor was also found to effect FFA removal of the feedstock when feedstock with zero percent moisture was reacted at 50 °C. An increase in the mixing rate increased the amount of FFA removal observed from a low of 3.8 ± 1.3% at 0 rpm to 79 ± 1.3% at 550 rpm. Based upon a review of available literature, no previous reports have examined the effect of mixing on the FFA removal with gel type resin. The increase in observed FFA removal is hypothesized to be caused by the increase in

collision frequency between the resin surface and FFA occurring due to the increased energy in the system.

3.2.3. Effect of wash solvent on resin regeneration Because deactivation of heterogeneous anionic resins by FFA adsorption onto quaternary ammonium sites is known to occur[29, 31, 50] resin regeneration for extended usage was of interest. Solvent washing was performed in order to remove oleic acid, glycerides (tri-, di-, and mono-), feedstock impurities, reaction intermediates, and reaction products that are either physically or chemically sorbed to the resin surface. Figure 3.3 shows the results of the solvent washing evaluation presented as the amount of FFA removal observed in a new 5% oleic acid in soybean oil reaction following a single wash step for each resin and for a non-washed resin.

The lowest amount of FFA removal (17 ± 2%) in the single cycle regeneration study was observed when no wash step was used. Without a solvent wash step, reusability of the resin was limited. However, following solvent washing the amount of FFA removal increased from 17 ± 2% without a wash up to 50 ± 4% FFA removal in wash solutions of MeOH and MeOH with 1 to 5% NaOH. Washing of exhausted resins with MeOH and 1% NaOH in MeOH produced statistically similar mean FFA removals ($p>0.05$). MeOH is hypothesized to regenerate the surface by reducing moisture and also acting as a solute for physically sorbed glyceride and FFA on the surface of the resin. Regeneration through reaction of surface bound triglycerides and FFA through esterification and transesterification is also possible if residual hydroxides or hydronium exists within the resin:feedstock mixture.

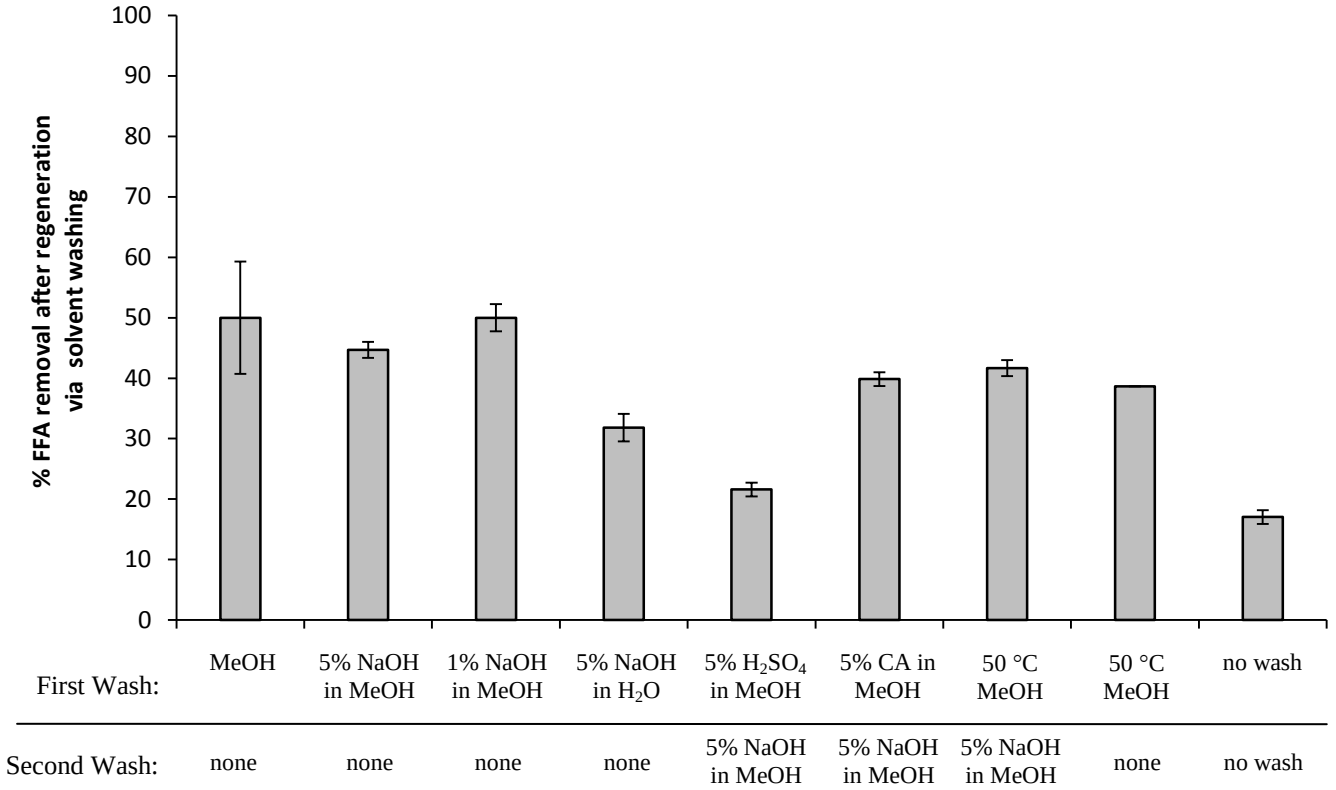

Figure 3.3 Deacidification (% FFA removal) following single cycle regeneration by washing resins with individual wash solvents or combinations of wash solvents (given below the bar). Error bars represent the error observed in triplicate reactors and CA represents citric acid.

When NaOH is added to MeOH, formation of sodium methoxide and the presence of hydroxide ions in the mixture are hypothesized to help establish a partial negative charge on the resin surface in addition to the effects of MeOH. The influence of NaOH on FFA resin surfaces has been similarly reported for basic resins[37]. Increasing the percent of NaOH in MeOH above 5% resulted in decreased FFA removal following the wash step which is hypothesized to be caused by saponification from residual sodium on or within the resin.

Increased FFA removal using the regenerated resin was observed when 5% NaOH in MeOH was used compared to 5% NaOH in water ($p<0.05$). Presence of moisture in the wash solution swells the acidic gel resins[30, 51] which is hypothesized to hinder FFA adsorption to the basic site. The basic functional site is also impacted by the presence of water in the wash solution[31].

Because a mixed bed ion exchange resin was used throughout the experiments, sequential solvent washes with acids followed by NaOH prepared in MeOH were investigated for their potential to regenerate the resin. Use of a hydrochloric acid wash followed by a NaOH wash in MeOH produced less FFA removal compared to use of citric acid wash ($p<0.05$). This finding may suggest that the stronger acid washing results in the generation of a salt layer around the resin matrix that diminishes its reusability. Adsorption of free ions of mineral salts present in the wash solution also deactivates acid functionality[1, 52].

3.2.4. Recoverable organics identified in wash solutions Two of the wash solutions used to successfully regenerate the resins were also screened to determine if recoverable

organics were present in the wash. The goal of the wash solution analysis was to identify organic products that were present in the wash, not to quantify the amount of recoverable organics present in the sample. Table 3.2 provides a listing of recoverable organics observed in the MeOH wash and 1% NaOH in MeOH wash solutions as identified through GC-MS analysis.

The wash solution analysis reveals that there are differences in the composition of recoverable organics when NaOH is present. MeOH is the primary component of the wash solutions as determined through peak area response. However, peaks identified as methyl esters are present in both wash solutions and could be recovered from the wash. Additionally, dodecanoic and undecanoic acids are present in the MeOH wash, but were not observed within the 1% NaOH in MeOH wash. Their absence from the 1% NaOH in MeOH wash solutions is likely due to the formation of additional esters in the wash solution with the presence of NaOH as a homogeneous catalyst. Understanding the composition of recoverable organics in the regenerative wash solutions is of interest, because the resulting wash solutions contain products of value that may become significant in volume based upon the volume of the oil being deacidified.

3.2.5. Effect of resin drying following wash step During the solvent wash experiments, washed resins were allowed to air dry for 18 hours between the wash step and their use in the single cycle regeneration experiments. Additional experiments were conducted to determine the effect of the resin drying duration following the wash step on FFA removal in the regeneration experiments. For the drying experiments, FFA

Table 3.2 Recoverable organics observed in resin wash regeneration solutions. The area % given in the table indicates the total percent of a compound's individual peak area within the chromatogram normalized to all the observed peaks in the injected sample. The area % is not a quantitative measure and is only included to show the relative relationship between the recoverable organics present in the washes.

Retention Time	Compound	MeOH Wash (area %)	1% NaOH in MeOH Wash (area %)
1.03	Methanol	55.03	69.22
18.97	decanoic acid methyl ester	np	1.6
20.91	hexadecadienoic acid dimethyl ester	0.82	2.44
21.32	9,12 octadecadienoic acid methyl ester	0.75	7.13
21.87	11,14,17-eicosatrienoic acid methyl ester	np	1.61
24.77	dodecanoic acid	1.22	np
27.64	undecanoic acid	1.64	np
28.25	15-tetracosenoic acid methyl ester	37.19	16.56
29.23	11,14-eicosadienoic acid methyl ester	3.35	1.44

np – not observed to be present

removal was compared based upon drying durations of 0, 9, and 18 hours. 1% NaOH in MeOH was the wash solvent used. Resins previously used to remove FFA from the prepared 5% oleic acid in soybean oil mixtures were washed and then dried at the specified duration with triplicate samples taken for each experimental data point.

FFA removal during the subsequent reuse of the dried resins was highest when the longest drying duration in this study was used. An increase in the resin drying time following the wash step increased the amount of FFA removal observed following single cycle regeneration. Observed FFA removal following the first step regeneration for drying durations of 0, 9, and 18 hours was 34±6.0%, 38±0.7%, and 50±2.2%, respectively. ANOVA testing resulted in rejection of the null hypothesis and Tukey's multiple comparison testing indicated that the mean concentrations of FFA observed in the feedstock following treatment with the resin were not statistically similar ($p<0.05$). The effect of resin drying on resin performance has been demonstrated in the past for S-DVB resins used for transesterification[38]. However, this past report looked at drying the resins to remove residual water present in the resin as delivered and not for the purposes of regenerating the resin following initial use.

3.2.6. Multicycle regeneration Figure 3.4 presents the results of FFA removal from fresh solutions of 5% oleic acid in soybean oil over three resin regeneration cycles with MeOH and 1% NaOH in MeOH used as wash solvents. All experiments were carried out at 50 °C for 2 hours at a mixing rate of 550 rpm without adding moisture externally to the prepared feedstock. Regardless of the wash solvent used, the capacity of the resin to remove FFA from solution decreased following each resin wash cycle (as

observed in Figure 3.4). Overall FFA removal was lower for the 1% NaOH in MeOH wash solution over multiple cycles. We hypothesize this difference is caused by saponification within the mixture on or at the surface due to the presence of Na^+ in solution after each successive resin cleaning. Although no visible soap formation was observed in the reacted mixture.

Despite a general decreasing trend, 40% of the initial FFA in the oleic acid soybean oil feedstock was removed from the mixture in the third regeneration cycle when MeOH was used as the wash solvent. Because no breakdown of the resin was observed, as has been reported earlier for acidic resins[21], the resin used in this study should be considered for feedstock deacidification. The ability to regenerate the resin will have positive benefits for reducing cost associated with using heterogeneous resins for deacidification.

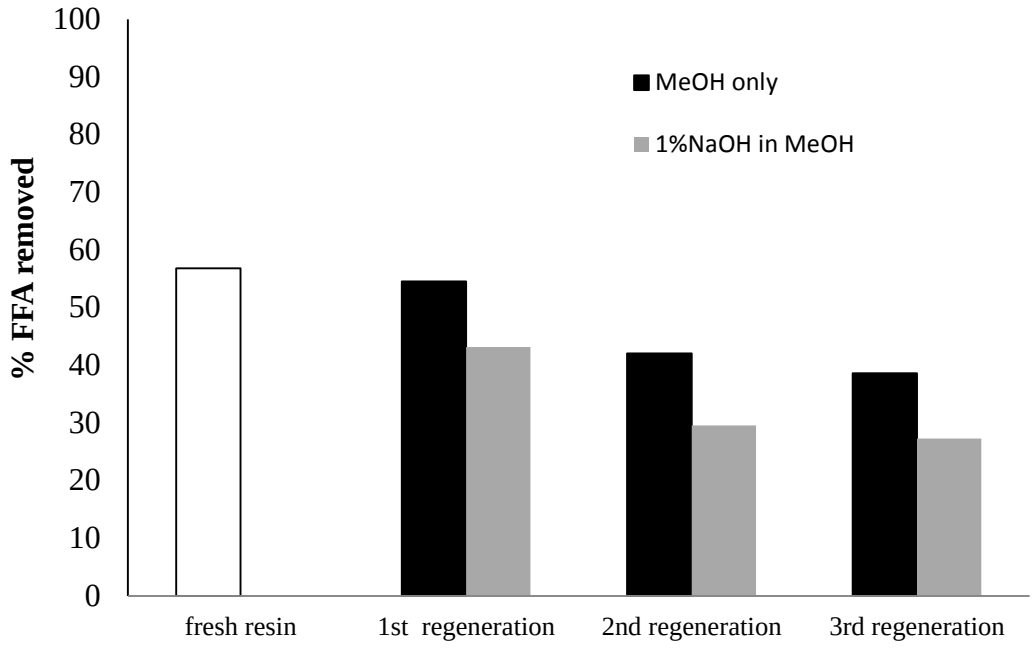

Figure 3.4 FFA removal from a 5% oleic acid in soybean oil mixture samples for fresh resin and resin regenerated up to three times using methanol or 1% NaOH in methanol as the wash solvent. The presented results reflect the mean FFA removal observed in triplicate samples. Fresh resins were not pretreated prior to use in the first deacidification and mean removal using the fresh resin is presented as a white bar.

3.2.7. Effect of feedstock on use of mixed bed ion exchange resins for deacidification

Experiments were conducted to determine the robustness of using the mixed bed ion exchange resin for deacidification of three WCO feedstocks. The feedstocks used were 1) WCO from a local University cafeteria with an initial acid value of 1.86% (unfiltered low FFA WCO); 2) WCO from a local fast food provider with an initial acid value of 23% (unfiltered high FFA WCO); and 3) unfiltered high FFA WCO with wax removed (filtered high FFA WCO). Wax was removed from the filtered high FFA WCO by gravity separation and filtration through 25 μm hardened ash less filter papers (Whatman 1541-185). Figure 3.5 presents the experimental results for deacidification of each feedstock using fresh resin and following a single step resin regeneration using a 1% NaOH in MeOH wash solution.

The resin was successful at reducing the acid value of the unfiltered high, filtered high and unfiltered low FFA WCO feedstocks by 41, 57, and 87% using fresh resin, respectively. The reduction in acid value was higher for use of fresh resin, but was observed for the washed resin following the first cycle of solvent washing. Statistically significant increases in FFA removal were also observed after removing wax from the unfiltered high FFA WCO. The improved performance following wax removal indicates that impurities within the feedstock have an effect on the surface of the resin. However, despite impurities within the feedstock, the mixed bed resin did deacidify the samples. This proof of concept in a highly impure feedstock demonstrates the promise of using

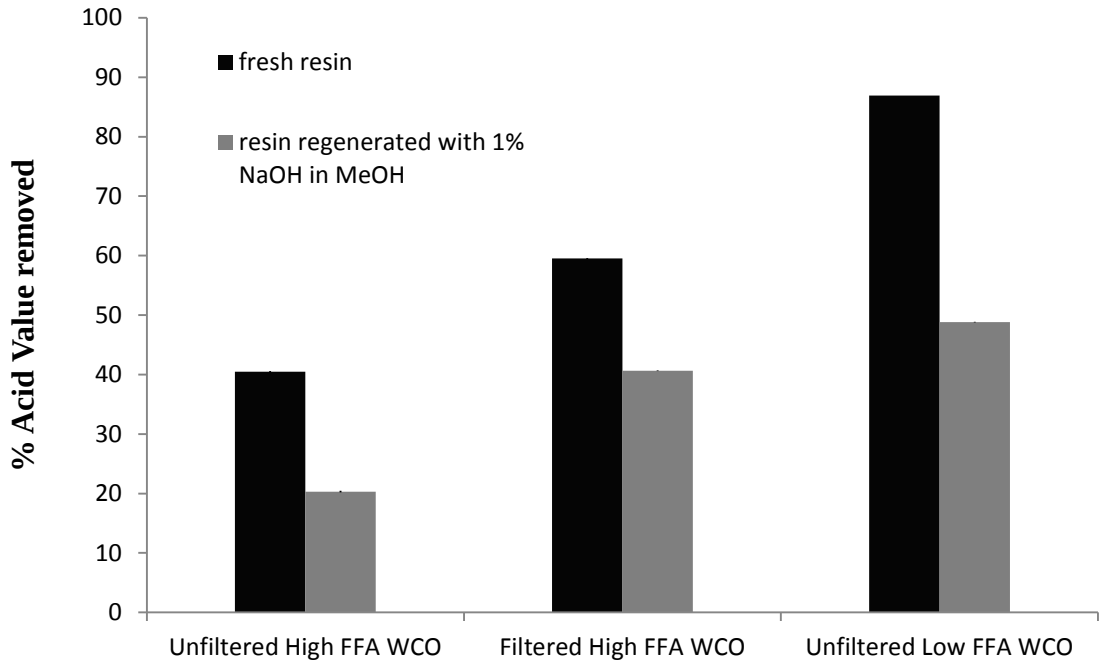

Figure 3.5 Deacidification of waste cooking oil (WCO) using Dowex Monosphere M-450 UPW. The initial acid value for the unfiltered high, filtered high, and unfiltered low WCO feedstocks was 23, 13.8, and 1.62, respectively. The presented results reflect the mean % acid value removal in triplicate reactors.

heterogeneous gel-type resins in the removal of FFA from a wide range of feedstocks and edible oils.

3.3 Conclusions

Dowex Monosphere MR-450 UPW mixed bed resin was used to deacidify laboratory prepared and locally available WCO feedstocks. Based upon the resulting experimental data, *deacidification using ion exchange resins is impacted by operational parameters including temperature, moisture content, mixing rate, and resin preparation*. The resin system handled up to 5% moisture content in the feedstock without impacting the amount of deacidification occurring during the reaction. The resin also was able to be regenerated following washing by various solvents. The solvents that resulted in the highest amount of FFA removal following a single step wash process were MeOH, 1% NaOH in MeOH, and 5% NaOH in MeOH. However, the presence of NaOH in the wash solvent produced statistically lower FFA removal in multiple step resin regeneration experiments, likely caused by the formation of soap on or near the surface of the resin. Recoverable organics including alkyl methyl esters and alkyl alcohols were observed in resin regeneration wash solutions. The resins were also demonstrated to deacidify WCO samples from local sources. Deacidification of WCOs increased in the presence of the resin when the WCO was first dewaxed and then deacidified using the resin.

4. MODEL TRANSESTERIFICATION OF SOYBEAN OIL FEEDSTOCKS WHEN AMBERLYST A26-OH IS USED AS A CATALYST (OBJECTIVE 2)

Objective 2 Hypothesis: *When methanol is present in excess the presence of FFA decreases the rate constant for methanol consumption*

4.1 Experimental Methods

4.1.1. Materials and reagents Amberlyst A26-OH (basic macroporous resin), 90% commercial grade oleic acid, and degummed soybean oil were purchased from Sigma-Aldrich (St. Louis, MO). HPLC grade MeOH was purchased from VWR International (Sugarland, TX). Nitrogen gas (99% purity) was purchased from BOTCO (Bryan, TX). Feedstocks consisting of degummed soybean oil or 5% oleic acid in degummed soybean oil (mass:mass) were prepared fresh daily and used in experiments.

4.1.2. Experimental setup Transesterification was investigated in a batch reaction system consisting of a glass flat bottom 250 mL round flask equipped with a vapor recovery traps sitting in a temperature controlled water bath (Figure 4.1). The feed for the system was either soybean oil or 5% oleic acid in soybean oil preheated to 100 °C to remove background moisture. Four grams of Amberlyst A26-OH (basic resin) were pre-soaked in methanol for 4 hours in the reaction flask prior to the reaction.

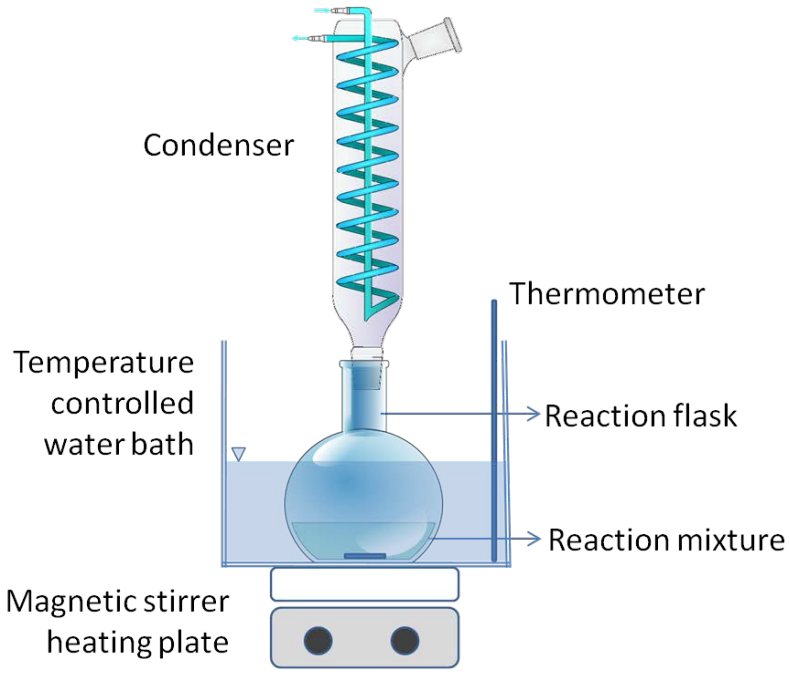

Figure 4.1 Batch reactor setup for transesterification experiments.

20 grams of the preheated feedstock was then poured in the flask containing the soaked resin. Separate reactors were used to investigate transesterification for soybean oil and 5% oleic acid in soybean oil at a 1:10 molar ratio of oil to methanol using Amberlyst A26-OH as a catalyst. All experiments were maintained at 50 °C while being stirred at 550 rpm using a magnet bar stirrer. The reaction systems were evaluated in duplicate for 0, 1, 2, 6, 12, and 18 hour reaction durations using sacrificial reaction volumes.

At each evaluated time step the appropriate reactors were pulled and centrifuged in order to separate the top fraction of reaction solution. The top fraction was then decanted and reduced to dryness under a gentle flow of nitrogen. The resulting dried mass from the top layer was recorded as the ester content produced in the reaction[53-55].

4.1.3. ER & LHHW surface reaction modeling Time series data from transesterification of feedstocks using Amberlyst A26-OH was evaluated against the Eley-Rideal and Langmuir-Hishelwood-Hougen-Watson reaction model to determine the kinetic model fitted parameters that describe the data and to help clarify the reaction process occurring on the surface of the resin. The models were also used to determine the impact of FFA on reaction kinetics. Figures 4.2 and 4.3 show the mechanisms for both the ER and LHHW models. Both models involve adsorption of methanol to the surface of the catalyst followed by a surface reaction. The primary difference between the two models is that in the ER model the surface bound methanol reacts with triglycerides in bulk solution, whereas in the LHHW model the triglyceride molecule first adsorbs to the surface of the catalyst and the two surface bound reactants combine

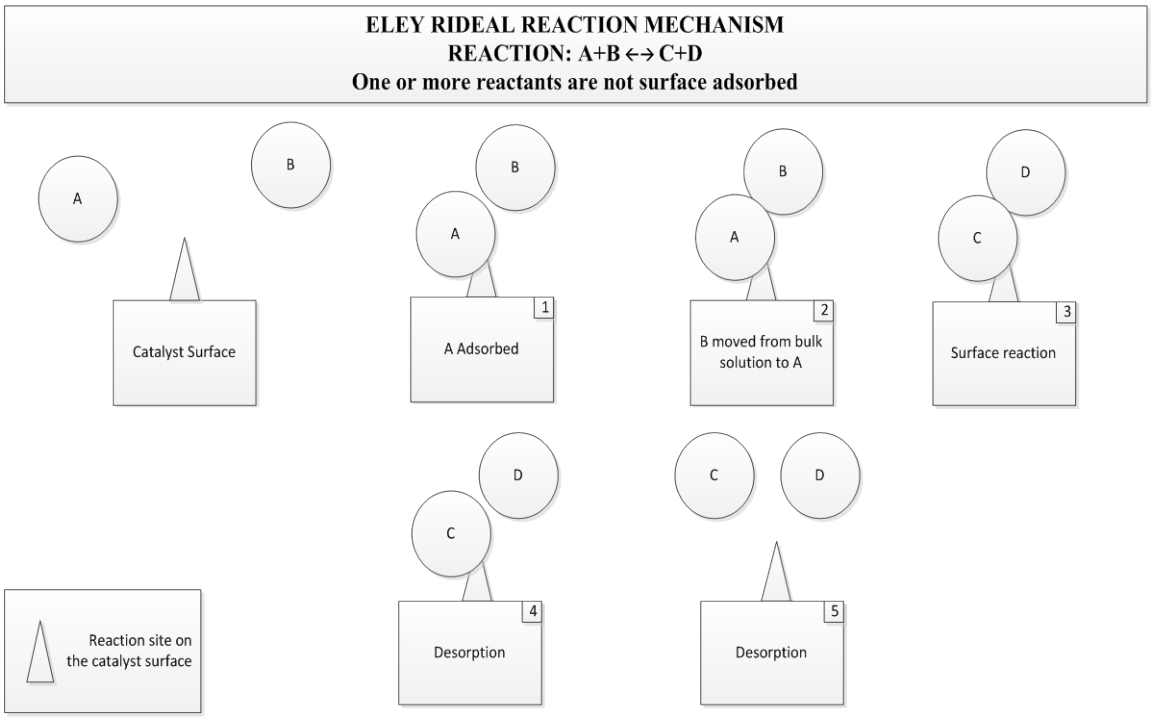

Figure 4.2 Graphical depiction of the reaction mechanism involved in the Eley-Rideal kinetic model.

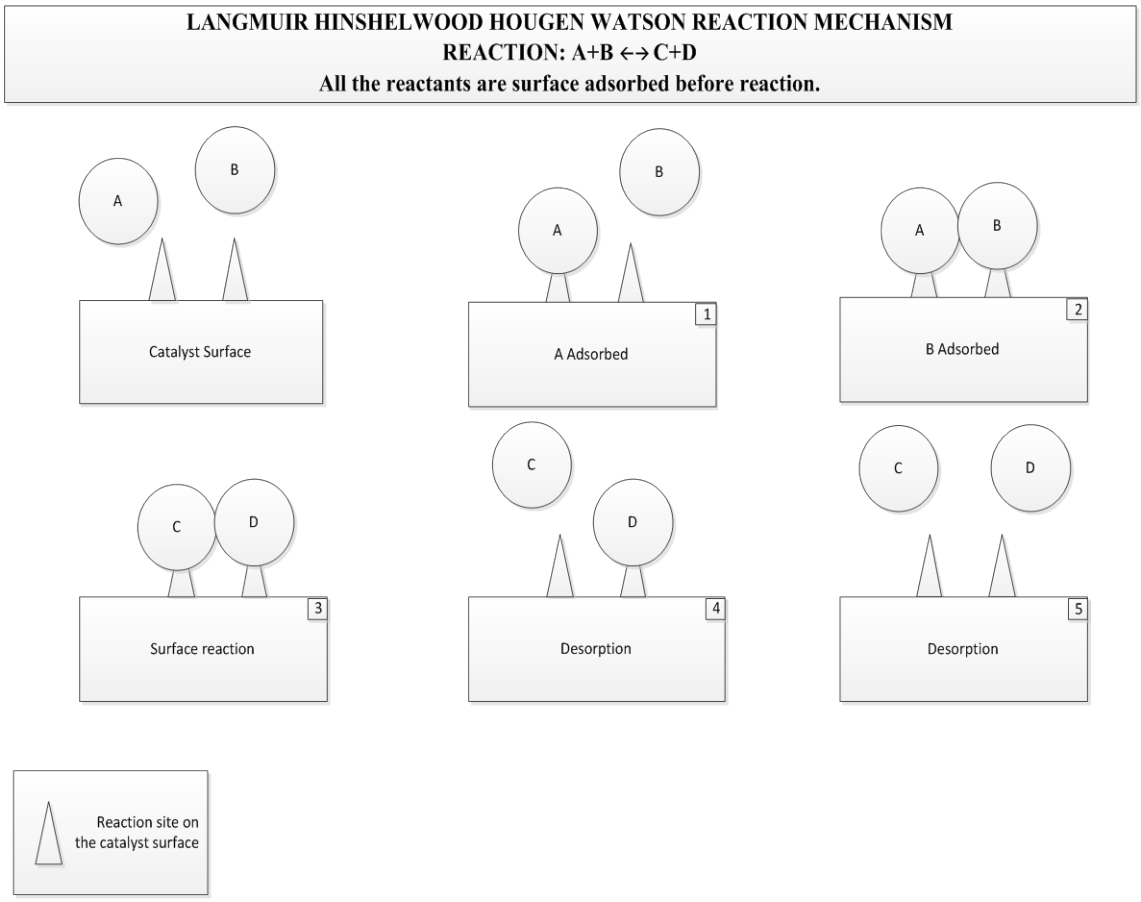

Figure 4.3 Graphical depiction of the reaction mechanism involved in the Langmuir-Hishelwood-Hougen-Watson kinetic models.

to form products. The ER and LHHW surface reaction models can also be written as a series of individual reactions steps according to Table 4.1.

While both the ER and LHHW model have been previously used to model transesterification on the surface of basic catalysts[53, 56-57], the models have not been developed for reaction on Amberlyst 26-OH. This presented research also applied a modified version of the models to account for the presence of FFA in feedstocks. The hypothesis was defined based upon the supposition that when FFA is in solution, the FFA competes for binding sites on the catalyst surface. The resulting modified ER and LHHW models were evaluated against the experimental data of transesterification of a 5% oleic acid in soybean oil feedstock with Amberlyst A26-OH. All model fitting of experimental data was based upon minimization of the root mean squared error (Δq) between predicted versus measured values and the resulting linear correlation coefficient (r^2). For the purposes of this modeling effort, Δq is defined by:

$$\Delta q = \sqrt{\frac{\Sigma\left[[E]_{t,experimental} - [E]_{t,modeled}\right)/[E]_{t,experimental}]^2}{(n-1)}}$$

where: $[E]_t$ = concentration of the esters at any time *t*; and

n = number of replicates.

Table 4.1 Stepwise reactions considered in ER and LHHW kinetic reaction models.

Reaction Step	**ER Model**	**LHHW Model**
Methanol Adsorption	$MeOH + * \underset{k-1}{\overset{k1}{\rightleftarrows}} MeOH^*$	$MeOH + * \underset{k-1}{\overset{k1}{\rightleftarrows}} MeOH^*$
Triglyceride Adsorption	n/a	$T + * \underset{k-2}{\overset{k2}{\rightleftarrows}} T^*$
Surface Reactions	$T + MeOH^* \underset{k-2}{\overset{k2}{\rightleftarrows}} E + D^*$ $D + MeOH^* \underset{k-3}{\overset{k3}{\rightleftarrows}} E + M^*$ $M + MeOH^* \underset{k-4}{\overset{k4}{\rightleftarrows}} E + G^*$	$T^* + MeOH^* \underset{k-3}{\overset{k3}{\rightleftarrows}} E^* + D^*$ $D^* + MeOH^* \underset{k-4}{\overset{k4}{\rightleftarrows}} E^* + M^*$ $M^* + MeOH^* \underset{k-5}{\overset{k5}{\rightleftarrows}} E^* + G^*$
Desorption	$D + * \underset{k-5}{\overset{k5}{\rightleftarrows}} D^*$ $M + * \underset{k-6}{\overset{k6}{\rightleftarrows}} M^*$ $G + * \underset{k-7}{\overset{k7}{\rightleftarrows}} G^*$	$D + * \underset{k-5}{\overset{k5}{\rightleftarrows}} D^*$ $M + * \underset{k-6}{\overset{k6}{\rightleftarrows}} M^*$ $G + * \underset{k-7}{\overset{k7}{\rightleftarrows}} G^*$ $E + * \underset{k-8}{\overset{k8}{\rightleftarrows}} E^*$

where MeOH = methanol; $*$ = surface site; MeOH* = methanol adsorbed on surface; T = triglyceride; D = diglyceride; M = monoglycerides; E = methyl ester; G = glycerol; T* = T adsorbed on surface; D* = D adsorbed on surface; M* = M adsorbed on surface; G* = G adsorbed on surface; E* = E adsorbed on surface; $k_{1 \text{ through } 8}$ are the forward reaction rate constants; and $k_{-1 \text{ through } -8}$ are the reverse reaction rate constants.

4.2 Results and Discussion

4.2.1. Transesterification of soybean oil with Amberlyst A26-OH Figure 4.4 shows the concentration of esters and glycerol generated during the course of an 18 hour reaction duration of Amberlyst A26-OH with soybean oil alone and with a 5% oleic acid mixture in soybean oil. The triglyceride concentration in the reactor was calculated based upon the difference between the known initial molar concentration of triglyceride in the feed and the weight of the evolved dried ester product. The methanol and glycerol concentrations within the reactor were calculated according to reaction stoichiometry.

4.2.2. ER and LHHW reaction modeling Through evaluations of the initial transesterification reaction rates on basic catalysts found in the literature, the ER and LHHW models were derived with methanol adsorption as the rate limiting step[53, 56, 58-60] . Methanol adsorption as the rate limiting step is further supported within the literature, because the reaction will not proceed without the formation of methoxide (a surface facilitated reaction with methanol)[58, 60-62] . The derived ER and LHHW models presented also assume that all surface reaction sites demonstrate equal reactivity towards methanol; adsorption is isothermal; and there are no internal or external mass transfer limitations.

Full derivations of both the ER and LHHW models are provided in Appendix A and B respectively. The final reduced versions of the model used in this research are presented in Table 4.2. Table 4.2 also provides the rate constant values resulting in the best fit of the data along with linear correlation coefficient (r^2) and the error associated with the best fit model and observed data (Δq).

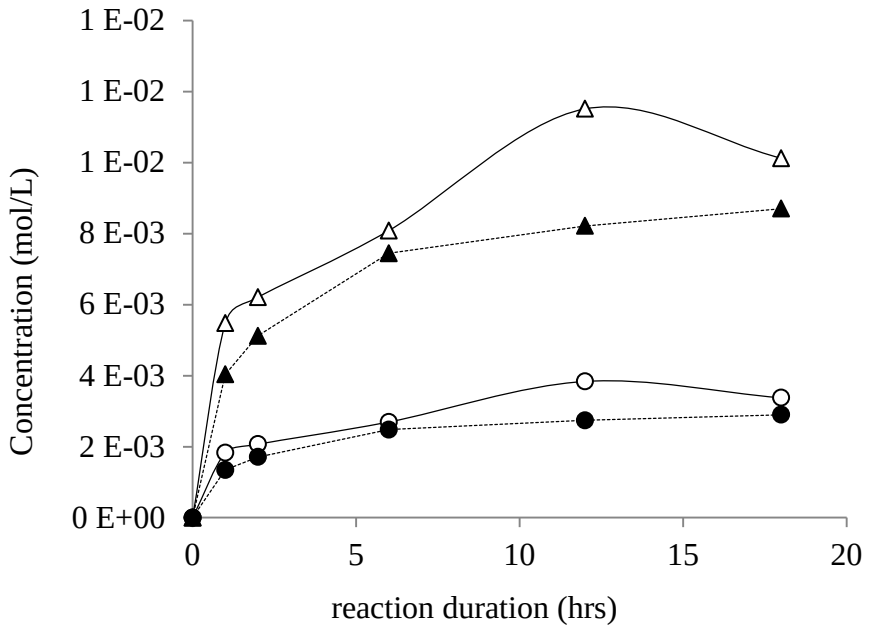

Figure 4.4 Concentration of observed esters (▲) and estimated glycerol (●) in the reactor over the course of the reaction of Amberlyst A26-OH with soybean oil alone (open markers and solid lines) and with a 5% oleic acid mixture in soybean oil (filled markers and dotted lines). Please note that lines represent trends, not a fit of the data.

Table 4.2 ER and LHHW kinetic models used to fit the experimental data presented with the best fit parameter values and resulting model statistical evaluation.

Model	Rate Equation	Parameter values	Units	r^2	Δq
ER kinetic model without FFA	$\frac{d[MeOH]}{dt} = \frac{-k[\mathrm{MeOH}]}{([1] + \mathrm{K_7[G]})}$	k = 7.48E-04 K_7=1.10E+04	1/hr L/mol	0.98	0.90
ER kinetic model with FFA	$\frac{d[MeOH]}{dt} = \frac{-\mathrm{k[MeOH]}}{(1 + \mathrm{K_7[G]} + \mathrm{K_8[FFA]})}$	k = 1.94E+00 K_7=2.15E+07 K_8=1.79E+04	1/hr L/mol L/mol	0.67	1.03
LHHW kinetic model without FFA	$\frac{d[MeOH]}{dt} = \frac{-\mathrm{k[MeOH]}}{(1 + \mathrm{K_2[T]} + \mathrm{K_6[E]} + \mathrm{K_9[G]})}$	k = 6.20E-02 K_2= 1.12E+02 K_6=2.99E+05 K_9=9.12E+01	1/hr L/mol L/mol L/mol	0.98	0.90
LHHW kinetic model with FFA	$\frac{d[MeOH]}{dt} = \frac{-\mathrm{k[MeOH]}}{(1 + \mathrm{K_2[T]} + \mathrm{K_6[E]} + \mathrm{K_9[G]} + \mathrm{K_{10}[FFA]})}$	k = 1.71E+00 K_2= 4.00E+03 K_6=2.09E+07 K_9=1.75E+07 K_{10}=1.50E+03	1/hr L/mol L/mol L/mol L/mol	0.66	1.06

Figure 4.5 provides the model fit showing the consumption of methanol as a function of time for each derived model. Based upon ER model fitting, the rate constant of methanol consumption was determined to be $2.08x10^{-7}$/sec with FFA absent and $5.39x10^{-4}$/sec when FFA is present. The LHHW model results in a rate constant of methanol consumption of $1.67x10^{-05}$ /sec and $4.75x10^{-04}$ /sec in absence and presence of additional FFA, respectively. Therefore, the presence of FFA in solution increased the rate constant for methanol consumption – contrary to the original hypothesized response.

Similar values, however, for this rate constant are noted by Kapil *et al.*[56] in their research investigating transesterification on hydrotalcite catalysts. They report a rate constant for methanol consumption in the range of $1x10^{-06}$ to $7x10^{-06}$/sec based upon the ER model and $1x10^{-02}$ to $9x10^{-03}$/sec for the LHHW model. Their reactions were run in the absence of FFA within a system with glyceryl tributyrate and methanol as the reactants with hydrotalcite catalysts[63]. Dossin *et al.*[60] also report on the reaction rate constant for methanol consumption during transesterification of triglyceride basic metal oxide catalysts. Their reported rate constant was 0.148 m^3/Kg.cat –s; compared to $1.6x10^{-06}$ m^3/Kg.cat –s for our catalyst. This comparison indicates that basic metal oxide catalysts have a much higher reaction rate during transesterification compared to the resins used in this study.

The data supports a rejection of the original hypothesis. This is a surprising outcome that allowed for further conceptualization of the reactions occurring on the surface. The original hypothesis was driven by the known adsorption interaction with FFA with the basic quaternary ammonium site on the resin. The adsorption was forecasted to block

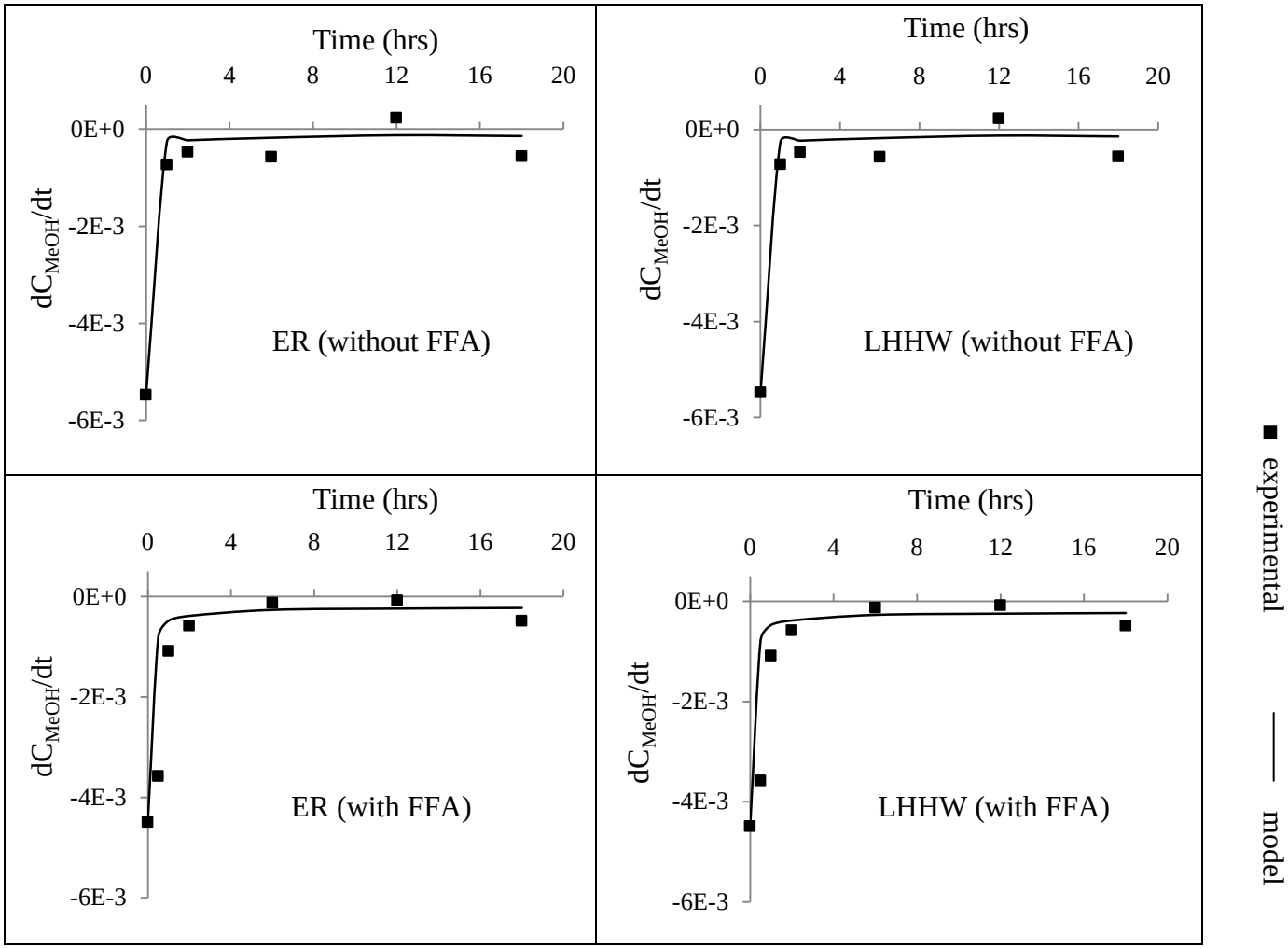

Figure 4.5 ER and LHHW kinetic models fit to the experimental methanol consumption data (mol/L·hr) for transesterification of soybean oil and a 5% oleic acid in soybean oil mixture with Amberlyst A26-OH used as a catalyst in the presence of MeOH.

the reaction of methanol with the basic site. Therefore, a decrease in the reaction rate was expected to account for lower consumption rates of methanol during the reaction. However, the opposite was observed and an increase in the reaction rate of methanol consumption was observed. Therefore, one of two possible mechanisms was proposed to explain the findings. Either methanol reacts with FFA or FFA facilitates the approach of triglyceride to the resin surface through decreasing the hydrophilic nature of the resin surface when FFA is surface bounded. A review of the literature did not yield indications that FFA would react with methanol without the presence of an acidic catalyst. Therefore, the difference in observed reaction rate constants for methanol consumption is most likely caused by the ability of FFA to foster triglyceride migration to the surface by lowering the hydrophilicity of the surface.

4.3 Conclusions

Transesterification of soybean oil with and without FFA present was investigated in the presence of methanol using Amberlyst A26-OH as a catalyst. In order to gain a better understanding of reaction mechanism occurring on the surface, both the ER and LHHW kinetic model were used to evaluate the data. The models were used to predict the change in methanol consumption over time (d[MeOH]/dt) in the reactor.

Both the ER and LHHW model were able to simulate the observed data. The addition of the FFA term into the model considerably improved the model prediction when FFA was present compared to when the model was used without a term for FFA. However, even with a term accounting for FFA, when FFA was present both models

resulted in over predicting the beginning phases of the reaction.

Additional evaluation of the models demonstrated that the reaction mechanism tends towards an ER hypothesized mechanism due to the presence of methanol in excess within the reactor. At excess levels of methanol the triglyceride component of the LHHW model plays a reduced role in the denominator of model equation. However, as the molar ratio of methanol to triglyceride decreases, the importance of triglyceride sorption on the surface of the resin increases. A similar phenomenon is observed as the ester yield increases; as increasing ester concentrations within the reaction system impact the denominator of the LHHW that are not important at low levels of ester in the reactor. Therefore, given the reaction conditions, the models indicate that methanol adsorption is the key step in reactions where methanol is present in excess and the ER model describes the reaction system. The proposed mechanism of transesterification on ion exchange resins when methanol is present in excess also supports the theory of transesterification of on basic catalysts present in the literature[50, 58, 60, 64].

Based upon ER model fitting, the rate constant of methanol consumption was determined to be 2.08×10^{-7}/sec with FFA absent and 5.39×10^{-4}/sec when FFA is present. This finding was contrary to the initially proposed hypothesis. Additional examination of the potential cause for the observed finding lead to the new theory that FFA promotes triglycerides approach to the surface. When FFA is adsorbed to the surface, triglyceride can interact with FFA through hydrophobic interactions. This interaction allows triglycerides to approach the surface more readily and the resulting transesterification reactions that take place lead to methanol consumption.

5. IN-SITU CONVERSION OF DRIED ALGAL BIOMASS TO BIODIESEL AND OTHER RECOVERABLE ORGANICS USING DOWEX MONOSPHERE MR-450 UPW AND A MIXTURE OF AMBERLYST A26-OH AND DOWEX MONOSPHERE M-31 AS CATALYSTS (OBJECTIVE 3)

Objective 3 Hypothesis: Simultaneous extraction and conversion of algae to recoverable organics can be achieved in a methanol:hexane solvent system with mixed bed ion exchange resins present as catalysts

5.1 Experimental Methods

5.1.1. Materials and reagents Dowex Monosphere MR-450 UPW (gelular resin), Amberlyst A26-OH (basic macroporous resin), Dowex Monosphere M-31 (acidic macroporous resin), methyl heptadecanoate (internal standard), 1 amp lipid mixture, oleic acid (≥ 99% purity) and TLC plates were purchased from Sigma-Aldrich (St. Louis, MO). Glacial acetic acid, HPLC diethyl ether, HPLC grade acetone, HPLC grade MeOH, HPLC grade hexane, and HPLC grade heptanes were purchased from VWR International (Sugarland, TX). Nitrogen gas (99% purity) was purchased from BOTCO (Bryan, TX). 500 mg silica SPE cartridges were purchased from SiliaPrep™ (Quebec, Canada).

Equal mass portions of Amberlyst A26-OH and Dowex Monosphere M-31 were combined to form the macroporous mixed bed resin used in the described experiments. Air and sun dried freshwater *Nannochloropsis oculata* was supplied by Algeternal

Technologies, LLC (Texas, USA) and was used as received without further drying. Prior to experimentation each algae sample was pulverized using a mortar and pestle.

5.1.2. Experimental setup Limited availability of dried algal biomass lead to a rethinking of the batch reactor system used for experiments carried out within Objective 3. The alternative reactor used for the algal biomass experiments consisted of a pre-cleaned 10 mL glass screw-top flat bottom vial containing a magnetic stirrer. Individual replicates contained one gram of pulverized algae with a specified volume of methanol:hexane co-solvent solution. The same setup was used to determine the extraction capacity of different solvent ratios of methanol:hexane and to evaluate in-situ transesterification.

The primary differences between the two evaluations included an addition of a known amount of either Dowex Monosphere MR-450 UPW (the gelular mixed bed resin system) or a mixture of Amberlyst A26-OH/Dowex Monosphere M31 (the macroporous mixed bed resin system) during the in-situ conversion investigations and secondary processing of the samples for the analysis. All reactions were carried out by placing the prepared vials in a water bath positioned on top of a heating-stir plate (Figure 5.1). Each individual reaction was carried out at 49 ± 1 °C at a constant mixing rate of 550 rpm for two hours.

5.1.3. Algae characterization The polar lipid fraction, non-polar lipid fraction, and lipid profiles within each fraction of both the air dried and sun dried *N. oculata* samples were characterized through solvent and solid phase extraction, gravimetric measurements, thin layer chromatography (TLC), and matrix assisted layer

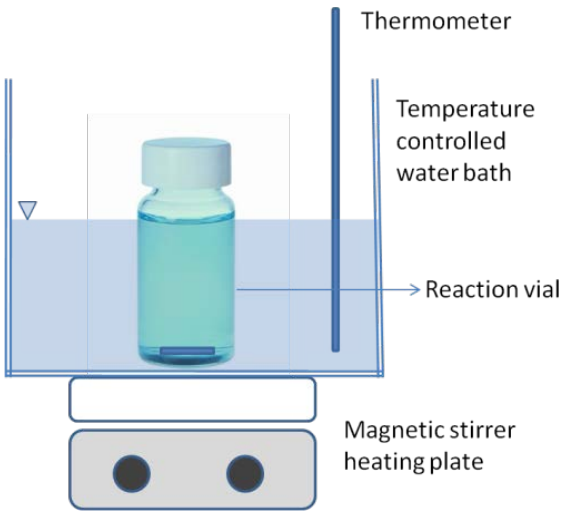

Figure 3

Figure 5.1 Batch reactor setup for in-situ algae conversion experiments.

desorption/ionization-time of flight (MALDI-TOF).

The polar lipid fraction within the algae was determined by extracting 1 g algae in 10 mL methanol by vigorously shaking for five minutes and then heating in a water bath for 30 minutes at 65 °C. The resulting supernatant was decanted and poured into a preweighed clean glass vial and then dried under a gentle stream of nitrogen. The weight of the remaining product was recorded as the total polar lipid fraction. The non-polar lipid fraction was determined in a similar manner, except 10 mL of a 3:1 hexane:chloroform solvent mixture was added following decantation of the methanol. The non-polar extraction also occurred in a water bath for 5 minutes at 65 °C. The polar and non polar dried fractions were then evaporated to dryness with nitrogen, resuspended in 0.5 mL solvent (chloroform for TLC and hexane for MADLI-TOF), and pooled together.

TLC and MALDI-TOF were then used to explore the lipid profile within the pooled extract. TLC plates were developed with a hexane:diethyl ether:glacial acetic acid (80:20:1) solvent mixture to resolve triglycerides, diglycerides, monoglycerides, and fatty acids. The developed TLC plate was then placed in a glass visualization chamber with iodine crystals in order to visualize the separated components. The area of the algae lipids spotted on the developed TLC plate was determined using Image J software by noting down spot pixel densities.

MALDI was performed on both SPE separated and non separated pooled lipid extracts to characterize the lipid profiles within the combined samples and within each fraction (polar and non-polar). SPE separation was achieved by loading 300 µL of the

pooled extract onto a 500 mg silica SPE cartridge that was pretreated with 1mL hexane. The cartridge was then eluted with 2 mL of 80:20:1 hexane:diethyl ether:glacial acetic acid to separate out the non-polar fraction. The collected fraction was reduced to dryness under a flow of nitrogen and reconstituted in 50 µL of acetone. The polar lipid fraction was eluded from the cartridge using 2 mL acetone and the eluent was collected. The two collected fractions (both in acetone) were then analyzed using MALDI-TOF to examine the lipid profile in each fraction. MALDI was performed on a Voyager STR equipped with a nitrogen laser (337nm, 3 ns pulse, and 20 Hz maximum firing rate). The instrument was operated in the reflectron modes with 2,4,6-trihydroxyacetophenone monohydrate as the matrix.

5.1.4. Co-solvent extraction capacity Triplicate samples of air dried algae were solvent extracted with different 4 mL ratios of methanol:hexane to evaluate the extraction capacity of the solvent systems used in this research. Because the goal of this research was to perform in-situ transesterification, a mixed solvent system was selected even though higher amounts of lipid could be extracted using a single solvent system. Therefore, to understand reaction yield the amount of extractable lipid realized with the co-solvent system used in the research also had to be determined. Co-solvent mixture ratios of methanol:hexane evaluated in this objective included 60:40, 40:60, and 20:80 (volume:volume). The reaction was carried out within the batch reactor system. The supernatant of each vial was collected via a syringe and passed through a 5-10 µm filter (Fisher Brand Qualitative P5) into a new pre-cleaned 10 mL vial. The amount of filtrate collected was weighed and the entire sample was evaporated. The resulting dried

sample was then weighed to determine the solvent extractable mass. The extractable yield was then presented as the solvent extractable mass normalized to the initial mass of the pulverized algae used in the extraction. Additional filtered supernatant for the 40:60 methanol:hexane extraction co-solvent was then stored for recoverable organic analysis.

5.1.5. In-situ conversion experiments In-situ conversion experiments were carried out in 4 mL of a 40:60 methanol:hexane co-solvent solution at a specified mass loading of mixed-bed resin operated at 50 °C at atmospheric pressure with a 550 rpm mixing rate. Initial time series evaluations of recoverable organics production as a function of reaction duration were carried out for duplicate one gram samples of sun dried pulverized algae in co-solvent with a 20% macroporous resin loading. The time series evaluation was conducted at intervals of 2, 4, 6, and 10 hours of reaction with and without the presence of resin. Additional in-situ conversion experiments described in the next section were carried out in order to develop a more detailed understanding of reaction parameters that improved the in-situ conversion yield. The supernatant from each batch reactor was syringe filtered and placed into a clean 4 mL vial and stored at 4 °C until analysis.

5.1.6. Effect of sonication, co-solvent volume, algae drying technique, and mixed bed resin structure on in-situ yield Experiments were carried out to determine the effect of 1) sonication, 2) co-solvent volume, 3) algae drying technique, and 4) mixed bed resin structure (gelular versus macroporous resin systems) on in-situ conversion yield. The effect of sonication was carried out by sonicating triplicate one gram samples of pulverized air dried algae in 4 mL of 40:60 methanol:hexane co-solvent. The samples

were sonicated for one hour and then reacted for one hour in the presence of 20%, 40% or 60% Dowex Monosphere MR-450 UPW resin loading.

The effect of co-solvent volume on in-situ yield was evaluated by increasing the 40:60 methanol:hexane co-solvent from 4 mL to 10 mL for a triplicate set of samples. One gram samples of pulverized sun dried algae in 4 mL and 10 mL of 40:60 methanol:hexane co-solvent were reacted in the presence of 20%, 40% or 60% Dowex Monosphere MR-450 UPW resin loading. The in-situ reaction yield of the increased co-solvent volume samples was then compared to the yield of non-sonicated sundried algae samples. The effect of the algae drying process on in-situ yield was evaluated by processing triplicate sun dried algae samples with 4 mL of 40:60 methanol: hexane co-solvent with a 20%, 40%, and 60% resin loading. The resulting in-situ yield was then compared to the yield observed for the air dried algae. Finally, the effect of mixed bed resin structure was evaluated by comparing the performance of the gelular against the macroporous mixed bed resin systems. One gram of pulverized algae was reacted with 20%, 40%, or 60% mixed bed resin loading in 4 mL of 40:60 methanol:hexane co-solvent. The resulting in-situ yields from both resin types are compared. The experiments were carried out for both air dried and sun dried algae.

Supernatant from each batch reactor was syringe filtered and placed into a clean 4 mL vial and stored at 4 °C until FAME analysis is conducted. The resulting FAME analysis of each sample was then used to calculate the in-situ conversion yield. The resulting yields for each parameter evaluation (sonication, co-solvent volume, algae drying technique, and resin structure) across resin loadings were compared for statistical

significance of the means using a student's t-test at a 95% confidence interval. All statistical analysis was carried out using SPSS version 20.

5.1.7. Ester content analysis The ester content in all evaluated samples was determined according to according to the European Standard method EN 14103[65, 66]. A Thermo Trace GC Ultra gas chromatograph (Thermo Electron Corporation) coupled to a Thermo DSQ II mass spectrometer was used to chromatographically resolve and quantify the ester content within injected samples using an internal standard method.

A 1 µL splitless injection was introduced on a Restek RxiTM-5ms column (60m x 0.25 mm ID x 0.25 µm film thickness) at an inlet temperature of 225 °C with helium as the carrier gas (flow rate of 1.5 mL/minute). The oven temperature gradient operated from 50 °C held for 5 minutes, ramped linearly to 320 °C at a rate of 20 °C/minute, and held at 320 °C for 5 minutes. The ion source and transfer line temperatures were maintained at 250 °C.

For analysis, 600 µL aliquots of syringe filtered supernatant from individual samples were transferred to a pre-cleaned 4 mL vial for evaporation under a gentle stream of nitrogen. The resulting dried extract mass was weighed and additional 50 µL aliquots of supernatant were transferred to the vial and re-evaporated until the final evaporated mass of the extracted sample is 10 mg. The 10 mg mass of extracted sample was then prepared for analysis to establish the recoverable organic content within the 10 mg of dried extract.

The 10 mg of dried extracts were reconstituted using 1 mL of *n*-heptane to establish a resulting solution concentration of 10 mg dried extract per mL *n*-heptane. Methyl

heptadecanoate was then spiked into the reconstituted extracts at a concentration of 0.04 mg/mL for use as an internal standard.

Xcaliber version 2.0.7 was used to calculate the peak area and height of the identified ester peaks. The concentration of each individual FAME within the reconstituted sample was then calculated according to:

$$[FAMEi] = \frac{[\mathrm{A}i - \mathrm{A_{ISD}}]}{\mathrm{A_{ISD}}} \times \frac{[\mathrm{C_{ISD}} * \mathrm{V_{ISD}}]}{\mathrm{m}}$$

where:

$[FAMEi]$ = mass of an individual FAME/mass dried reaction product

Ai = peak area of all the FAME including internal standard

A_{ISD} = peak area of the internal standard methyl heptadecanoate

C_{ISD} = concentration of Internal standard methyl heptadecanoate solution

V_{ISD} = volume of Internal standard solution added

m = weighed mass of analyzed sample

The mass of esters produced per mass of algae (mg_{ester}/g_{algae}) was then determined according to:

$$= \frac{[\Sigma(\mathrm{FAME}i)] \times \frac{\text{weight } dried\ reaction\ product}{evaporated\ supernatant\ volume} \times total\ supernatant\ volume}{\text{sample algae weight}}$$

The resulting in-situ conversion yield is then determined according to:

$$\text{In-situ Yield (\%)} = 100 \times \frac{\text{ester weight}}{\text{algae weight} * \text{algae extractable yield}}$$

5.1.8. Identification and analysis of additional recoverable organics Analysis of other recoverable organics present in the reaction solution was conducted similarly to the analytical method used to quantitate esters. This method was considered semi-quantitative in nature, because the response factors for all recoverable organics identified within a reaction solution were not known against the internal standard.

The peak area and peak height of identifiable peaks were then used to approximate a concentration of the identified analyte within the reaction solution assuming a uniform response against the internal standard. Because of the semi-quantitative nature of the method and the assumption of uniform response factors, the identified compounds were grouped into type prior to determining the percent of each observed group in a sample. The groups included alcohols, aldehydes, and alkanes (broadly defined). Subgroups of particular interest included esters and phytols. The content of each group or subgroup

within a sample was then calculated according to the calculation previously described in Section 5.1.7 for calculating the ester content.

5.2 Results and Discussion

The following describes the results of algae characterization:

1. *Gravimetric Determination of Polar and Non Polar Fraction.* The content of polar lipids and non-polar lipids in air dried *N. oculata* was determined to be 122.8 and 12.7 mg_{lipid}/g_{algae}, respectively. The observed content is higher than the polar and non-polar lipid mass fraction of sun dried *N. oculata*, which was estimated to be 104.6 and 10.1 mg_{lipid}/g_{algae}, respectively. Converti *et al.*[67] has reported similar total lipid content 134 mg_{lipid}/g_{algae} in *N. oculata* at growth conditions of 15 $^{\circ}C$ and 0.150 g/L $NaNO_3$.

Because both the air and sun dried algae used in our experiments were grown under the same conditions, the effect of the drying method was evident within our data set. Literature sources also demonstrate that sun drying breaks down lipids within algae[36, 68] . The total mass of polar and non-polar lipids present in each algae can also be used to determine the theoretical yield of esters that could be realized. Based upon total mass, the resulting yield is 142.0 mg and 120.0 mg ester/gm air and sun dried algae respectively.

2. *TLC Analysis of Pooled Polar and Non-Polar Extract.* Figure 5.2 provides a representative TLC plate observed during algae analysis. The analysis was repeated on two occasions to determine the triglyceride, diglycerides, monoglycerides, and fatty acid content within the samples. Table 5.1 provides the results of the TLC ImageJ

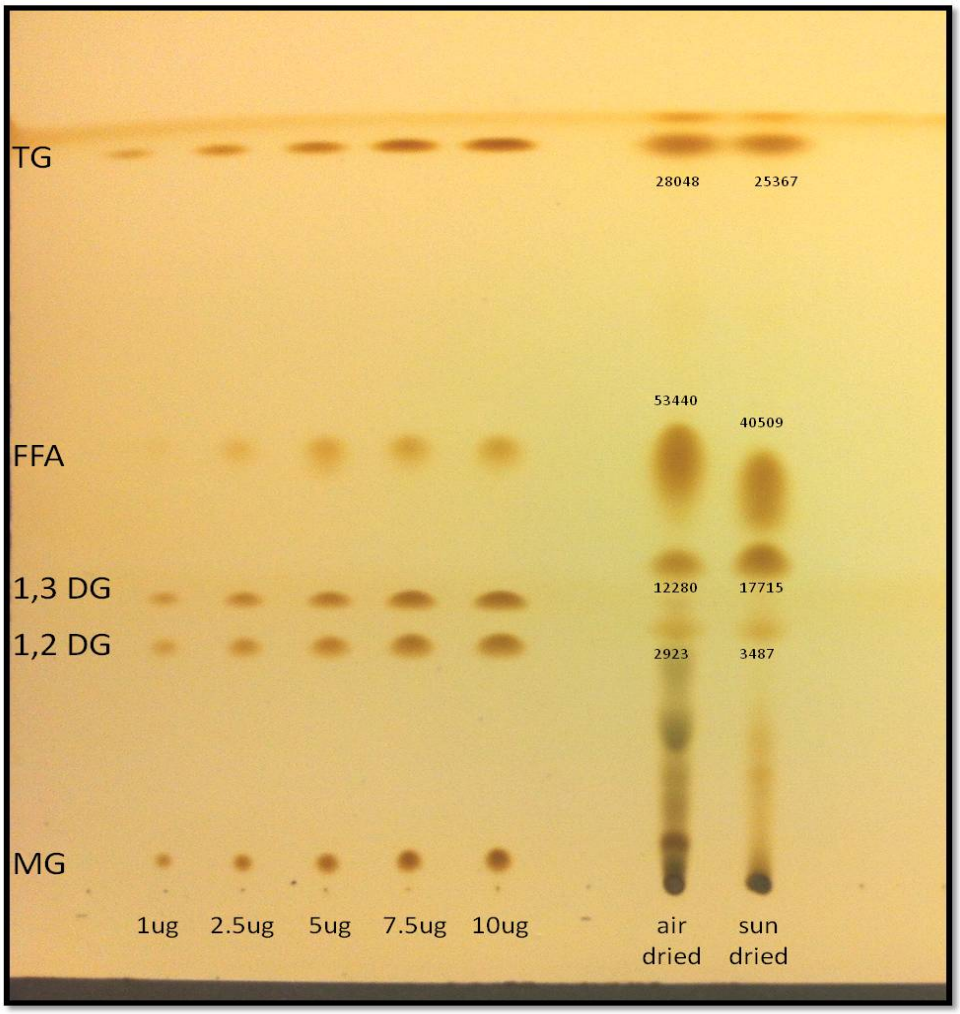

Figure 5.2 Developed TLC plate showing distribution of lipids for air dried and sun dried *N. oculata*.

Table 5.1 Composition of lipid fractions in algae based upon TLC analysis.

Lipid Type	Air Dried Fraction (mg_{lipid}/g_{algae})	Sun Dried Fraction (mg_{lipid}/g_{algae})
Triglycerides	15.6	14.1
FFA	49.4	37.5
1,3 Diglycerides	10.2	14.7
1,2 Diglycerides	2.30	2.80
Monoglycerides	N/A	*N/A

*N/A - Not Available

analysis of pixel densities presented on a mass basis. Beal *et al.*[69] validated the use of ImageJ software for determination of various algae lipid composition. This extraction and video imaging technique was also reported earlier for phospholipid presence and quantification in other biological samples[70].

TLC analysis showed a distribution within the samples between triglycerides (20% of lipid composition for both samples), diglycerides (16% of lipid composition for air dried and 25% for sun dried algae), and fatty acids (64% of lipid composition for air dried and 54% for sun dried algae). Monoglyceride content was not included within the distribution (and calculated percentages); however it appears that monoglycerides was prevalent in greater amounts in the air dried sample based upon TLC spotting analysis.

3. *MALDI-TOF Analysis of Separated Polar and Non-Polar Lipid Extract.* MALDI-TOF analysis was used to identify the composition of lipids within the separated fractions of the extracts. Figure 5.3 provides the mass spectra of both the polar and non-polar lipid extracts. Please note that given mass/charge ratios are provided with the sodium adduct present [mass+Na^+]. Examination of the MALDI-TOF spectra shows observable differences between the two extracts. The spectra show triglyceride peaks (nominal *m/z* 543.7, 549.8, 591.9, 601.8, 686.1, 744.1, 904.1, 911.1, and 9401.1) present in the non-polar fraction, but absent in the polar fraction. Peaks representing the fatty acids (nominal $m/z < 400$) appear in both spectra; however, these peaks are more pronounced in the polar spectra. Identified fatty acids include hendecanoic acid

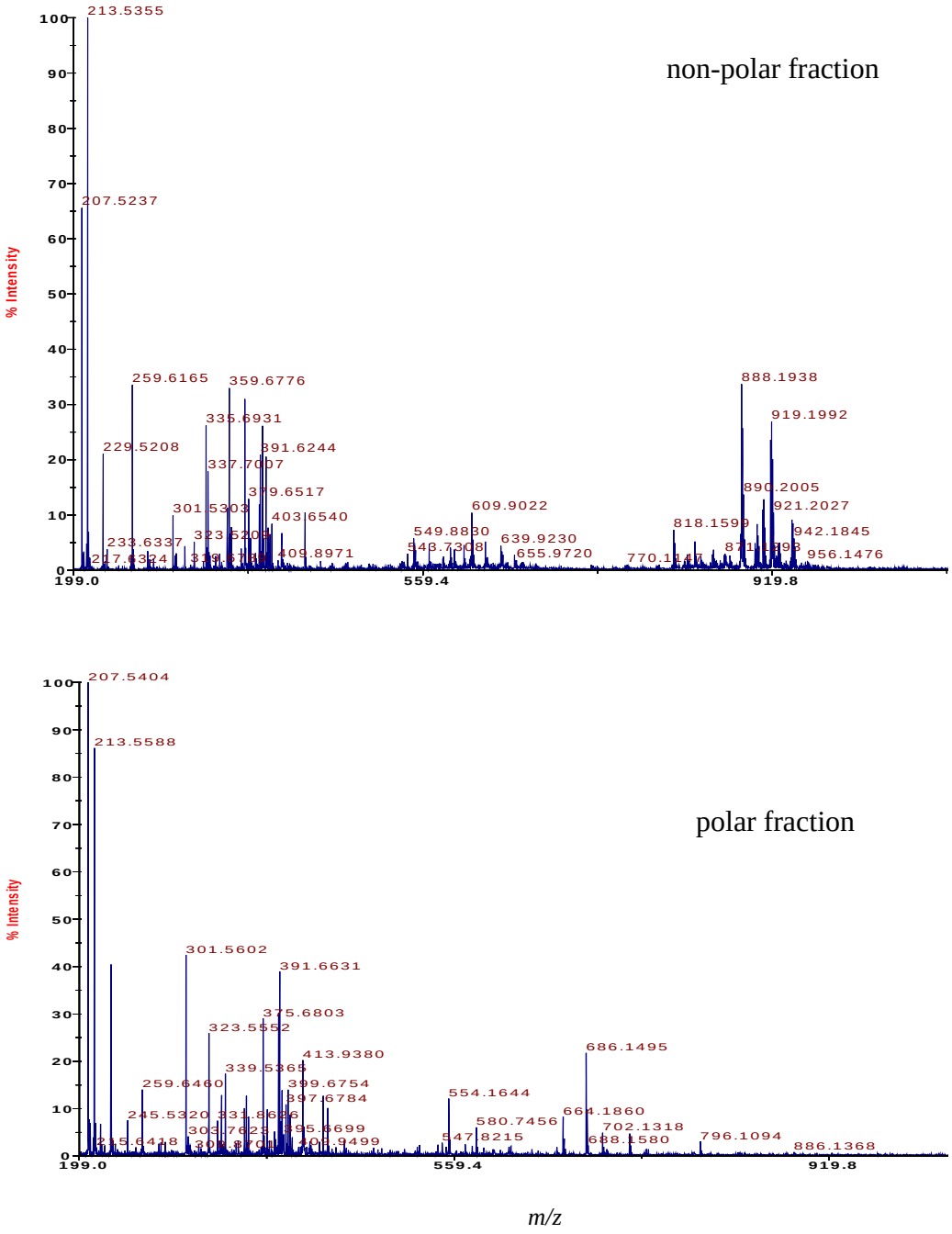

Figure 5.3 Representative MALDI-TOF mass spectra for non-polar and polar lipid SPE extracts. Shown spectra are from air dried algae following SPE extraction.

(nominal *m/z* 207.5), c-9,12-octadecadienoic acid (nominal *m/z* 301.6), eicosanoic acid (nominal *m/z* 335.7), and tricosanoic acid (nominal *m/z* 375.6). Because a TOF instrument was used, spectral libraries were used to determine the actual structure of the triglycerides and fatty acids present in the extracts based upon exact mass. The composition profile based upon spectral library[71-73] analysis for the polar and non-polar extracts are provided in Table 5.2.

5.2.1. Co-solvent extraction capacity The co-solvent extraction capacity for air dried algae was determined to be $5.5x10^{-2} \pm 1.7x10^{-3}$ g_{lipid}/g_{algae} for the 60:40 MeOH:hexane co-solvent, $6.0x10^{-2} \pm 9.1x10^{-3}$ g_{lipid}/g_{algae} for the 40:60 MeOH:hexane co-solvent, and $1.4x10^{-2} \pm 6.8x10^{-4}$ g_{lipid}/g_{algae} for the 20:80 MeOH:hexane co-solvent. The highest lipid extraction occurred for the 40:60 MeOH:hexane co-solvent system. A 40:60 MeOH:hexane solvent ratio was also observed to yield the highest lipid extraction in Li *et al*.[34] work with *Chlorella pyrenoidosa*. Therefore, the 40:60 MeOH:hexane co-solvent system was used for the remainder of the experiments. The 40:60 MeOH:hexane co-solvent extraction capacity for sun dried algae, sonicated air dried algae, and for 10 mL extraction of sun dried algae was determined to be $3.9x10^{-2} \pm 9.1x10^{-3}$, $9.85x10^{-2} \pm 3.5x10^{-3}$, and $19x10^{-2} \pm 4.2x10^{-3}$ g_{lipid}/g_{algae} respectively.

The resulting co-solvent extraction capacity can also be used to evaluate the maximum practical yield based upon the extraction solvent used in the system. The mean practical transesterification yield from the algae used in our experiments was calculated to be 63 mg_{ester}/g_{algae} for air dried and 41 mg_{ester}/g_{algae} for sun dried. This amount is 44% and 34% of the theoretical yield (respectively) that was based upon the

Table 5.2 Lipid profile within non-polar and polar SPE extracts as determined through MALDI-TOF.

Extract fraction	Identified Components (nominal *m/z*)
Polar	Fatty acids hendecanoic acid (207.5) c-9,12-octadecadienoic acid (301.6) tricosanoic acid (375.6) Diglycerides CyM, LaCa, or PCo (433.5) Triglycerides CoCoCy, BuBuLa,VVCa or CyCyV (427.8) SSCo, PPCa, LaLaS, or MMM (744.1)
Non-Polar	Fatty acids hendecanoic acid (207.5) c-9,12-octadecadienoic acid (301.6) tricosanoic acid (375.6) eicosanoic acid (335.7) Diglycerides LnS or LO (623.9) Triglycerides VVLn (543.7) VVS, CoCoP, EnEnM, CyCyLa, CaCaCy, BuBuA, or LaLaBu (549.8) LaLaEn (591.9) EnEnL (601.8) LLS or OOL (904.1) SSO (911.1) SSA or AAP (940.1)

Abbreviations are:
A= eicosanoic acid, Bu=butanoic acid, Ca= decanoic acid, Co= hexanoic acid, Cy= octanoic acid, En= heptanoic acid, L= c-9,12-octadecadienoic acid, La= dodecanoic acid, Ln= c-9,12,15-octadecatrienoic acid, M = tetradecanoic acid, O=c-9-octadecenoic acid, P= hexadecanoic acid, S= octadecanoic acid,V= pentanoic acid.

total lipid extraction using methanol and a mixture of hexane and chloroform. The 40:60 MeOH:hexane solvent extraction mixture used for this research provides methanol for the catalysis reaction, but reduces the amount of extractable material available for the reaction.

5.2.2. In-situ conversion of algal biomass to esters Table 5.3 provides a summary of factors effecting the in-situ conversion of algae into esters on a mass basis. The method used to dry the algae (forced air versus sun drying), the structure of the resin (gelular versus macroporous), sonication, and solvent volume were all observed to have an effect on mean ester content of the reaction product solution. The observed difference in ester yield as a function of algae drying was caused because sun drying algae breaks down triglycerides to form more free fatty acids within the dried algal biomass[36]. Table 5.4 provides the resulting percent in-situ yield under the same reaction conditions for air and sun dried algae.

Table 5.3 Ester produced per dry weight of air and sun dried algae (mg_{ester}/g_{algae}) at different catalyst loadings.

Experiment	Resin Type	Algal Drying Method	Solvent Volume (mL)	Sonicated	Catalyst Loading (%) 20	40	60	Statistically Similar Means
Effect of algae drying	gelular	air	4	No	37.2	9.7	1.0	No
	gelular	sun	4	No	1.4	0.9	0.2	
	macroporous	air	4	No	20.3	9.8	3.2	No
	macroporous	sun	4	No	8.9	4.0	2.4	
Effect of resin type	gelular	air	4	No	37.2	9.7	1.0	No
	macroporous	air	4	No	20.3	9.8	3.2	
	gelular	sun	4	No	1.4	0.9	0.2	No
	macroporous	sun	4	No	8.9	4.0	2.4	
Effect of sonication	gelular	air	4	Yes	39.8	24.5	14.6	No
	gelular	air	4	No	37.2	9.7	0.6	
Effect of Solvent	gelular	sun	10	No	2.5	1.4	1.4	No
	gelular	sun	4	No	1.4	0.9	0.2	
					(ester produced, mg_{ester}/g_{algae})			

Table 5.4 Percent in-situ reaction yield at different catalyst loadings for air and sun dried algae.

Resin Type	Algal Drying Method	Solvent Volume (mL)	Catalyst Loading (%)		
			20	40	60
gelular	air	4	59.3	15.4	1.6
gelular	sun	4	3.4	2.2	0.5
macroporous	air	4	32.4	15.4	5.1
macroporous	sun	4	21.9	9.8	6.0
			Percent in-situ reaction yield		

Sonication and solvent volume were both observed to have a statistically significant effect on ester yield during in-situ processing of algae with the mixed bed resin system. Sonicating the algae in the presence of solvent and increasing the solvent volume both acted to increase the amount of lipids released into the bulk solution by increasing lipid extraction efficiency[74-76]. Another interesting observation was a statistically significant decrease in ester yield as the catalyst loading increased. At first this decreasing trend was proposed to be caused by esters either adsorbing onto the resin or absorbing into the resins. While this may be occurring, the data also indicated that the esters could be reaction intermediates in the pathway to other organics as esters appear to undergo additional reaction with the resin.

In consideration of both sorption and reactive intermediates as likely explanations for the decreasing trend of ester production as a function of catalyst loading, the reactive intermediate explanation appears to be more plausible as the ester yield decreases more for gelular resins than for macroporous resins as a function of catalyst loading. Because gelular resins have limited porosity to facilitate pore site reactions, if sorption were of significance in this system the gelular resin should have higher ester yield at higher catalyst loadings. However, based upon the data the reverse appears to be true. Presence of additional ester based metabolites was also observed in the reaction solution; favoring that the observed trend is based upon the role of esters as a reactive intermediate. However, additional future research can and should be carried out to confirm this conclusion.

5.2.3. In-situ conversion reaction products Figure 5.4 and Table 5.5 provide information concerning the reaction products observed during the in-situ reaction of *N. oculata* with mixed bed resin at a 20% catalyst loading at 50 °C and 550 rpm in the batch reaction system. The evolved products show formation of esters, alcohols, and ketones. Interestingly, phytol represents one of the largest single peaks in the system occurring at a retention time of approximately 17.33 minutes. The unexpected presence of phytol, other alcohols, and ketones within the reaction solution pointed out the complexity of the underlying multi-component reactions occurring in the system. Future additional dissertations could examine the reaction of each individual product with the acidic or basic functional group in the mixed bed system. However, this is beyond the scope of this proposed work.

Figure 5.5 provides the change in relative contribution of each ester peak during the course of the reaction for a 20% resin loading. C_{11}-C_{15} esters are present in the reaction solution at each time step, but at very low concentrations (below 1% of the total ester content). The reaction solution was dominated by the presence of C_{18} esters and also contains C_{16} esters. C_{18} esters decreased over time, hinting at the additional reactivity of the esters to the mixed bed resin.

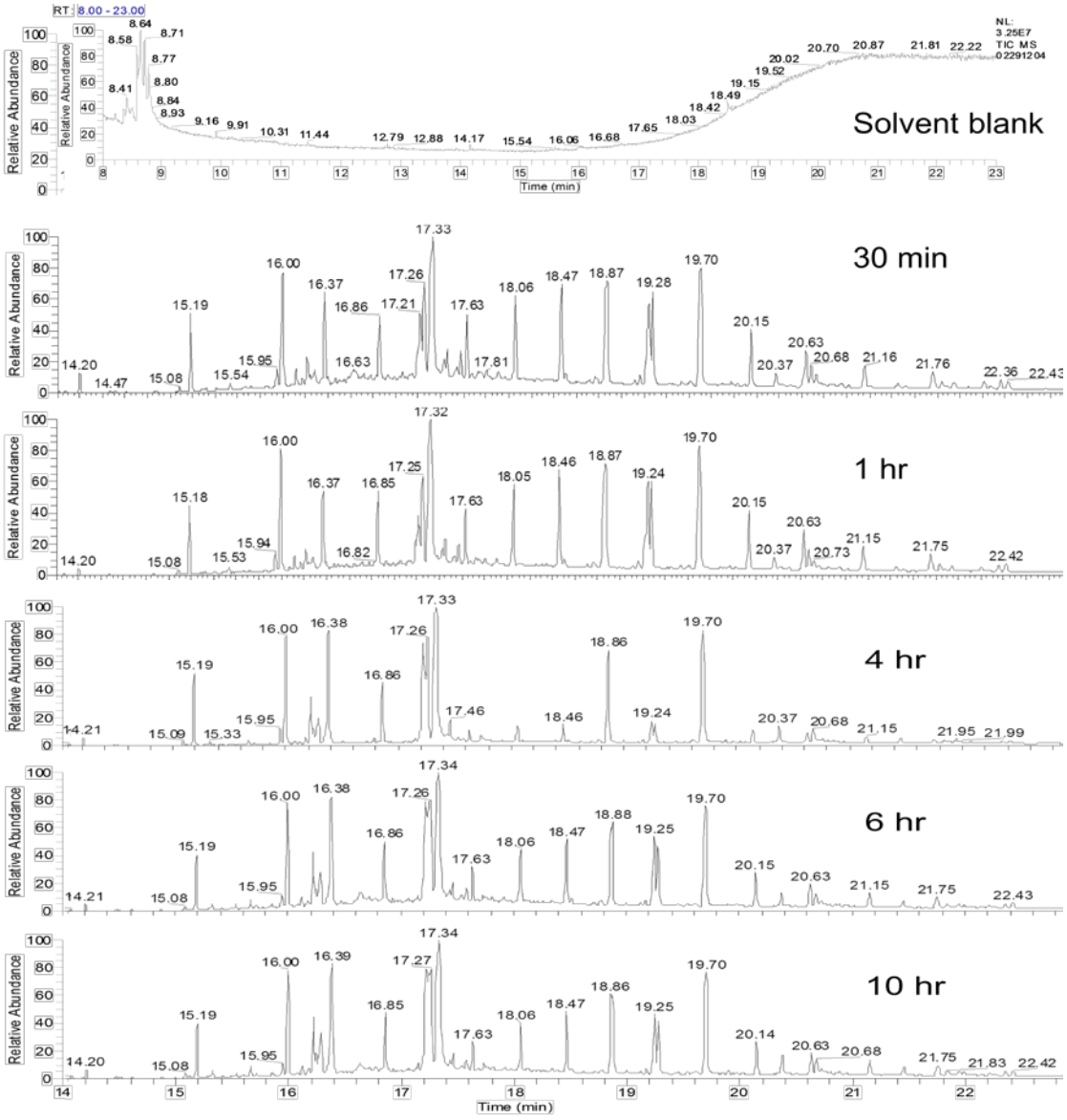

Figure 5.4 Representative chromatograms of reaction products over the course of the reaction (30 minutes, 1 hour, 4 hours, 6 hours and 10 hours) of the mixed bed resin systems with *N. oculata* at 20% catalyst loading, at 50 °C, 550 rpm, and in a 40/60 methanol hexane co-solvent.

Table 5.5 Representative identified reaction products of in-situ reaction of *N. oculata* with 20% mixed bed resin in methanol:hexane co-solvent.

Peak Retention Time (min)	%Area	Identified Analyte
14.13	0.01	β-ionone
14.26	0.37	butylated hydroxytoluene
15.14	0.08	3-heptadecene
15.24	2.57	heptadecane
15.33	0.04	2,6,10-trimethyltetradecane
15.37	0.59	tetradecanoic acid methyl ester
15.65	0.51	4,8,12-trimethyl tridecanoic acid methyl ester
15.71	0.09	pentadecanoic acid methyl ester
15.76	0.02	12-methyl tetradecanoic acid methyl ester
15.91	0.03	pentadecanoic acid methyl ester
16	0.56	3,7,11,15-tetra methyl-2-hexadecene-1-ol
16.05	7.12	2-pentadecanone
16.13	0.11	3,7,11,15-tetramethyl-2-hexadecen-1-ol
16.22	0.23	3,7,11,15-tetra methyl-2-hexadecene-1-ol
16.27	2.35	unidentified peak
16.3	0.43	7,10-hexadecadienoic acid methyl ester
16.34	1.54	7,10,13-hexadecatrienoic acid methyl ester
16.43	15.23	hexadecanoic acid methyl ester
16.49	0.07	unidentified peak
16.55	0.07	unidentified peak
16.83	0.13	unidentified peak
16.9	1.15	heptadecanoic acid methyl ester*
17.2	0.09	10,13-octadecadiynoic acid methyl ester
17.27	8.9	9,12-octadecadienoic acid methyl ester
17.29	4.12	9-octadecenoic acid methyl ester
17.31	10.64	9,12,15-octadecatrienoic acid methyl ester
17.34	37.89	phytol
18.08	0.12	unidentified peak
18.9	1.74	unidentified peak
19.74	2.96	unidentified peak
20.44	0.18	unidentified peak

* internal standard

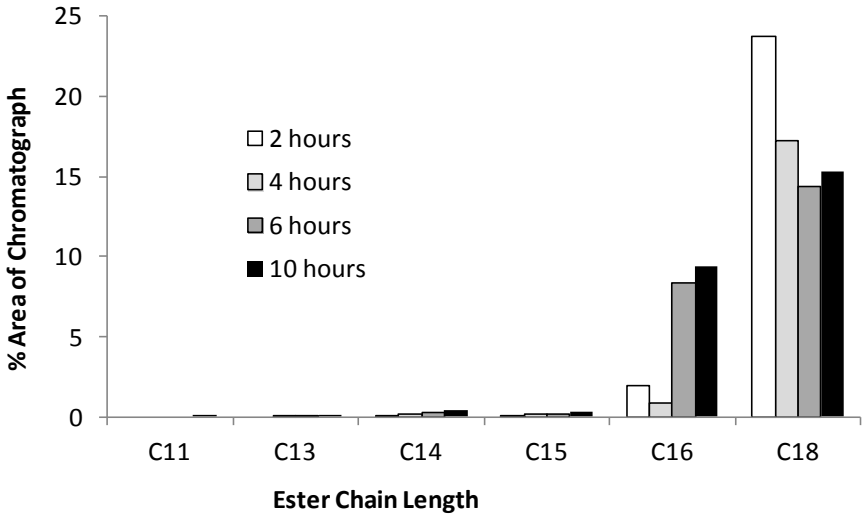

Figure 5.5 Changes in ester formation over time during the in-situ conversion of *N. oculata* with mixed bed ion exchange resin.

One possible explanation for the decrease of esters observed in the reactors over time is the further reaction of esters with the acidic functional group on the resin to form alcohols and ketones[77-78] . These reaction products, shown in Figure 5.6, were also present in the reaction solutions and increased in concentration at each time step. Additional ester loss in the reaction is also proposed to occur due to sorption of the esters to the resin itself.

5.3 Conclusions

In-situ conversion of algal biomass to biodiesel and other recoverable organics was investigated. Based upon the resulting experimental data, *simultaneous extraction and conversion of algae to recoverable organics can be achieved in a methanol:hexane solvent system with mixed bed ion exchange resins present as catalysts.* The reaction of air or sundried algae with gelular or macroporous mixed bed resin systems resulted in the formation of esters and other reaction products in as few as 30 minutes. The highest reaction yield of esters (up to 60% yield) occurred within 2 hours following the reaction of 20% gelular type mixed bed resin (by weight) with air dried *N. oculata* at 50 °C and a mixing rate of 550 rpm. The algae drying method, the structure of the resin, sonication, and solvent volume were all observed to have an effect on mean ester content of the reaction product solution. The experimental data also indicated a decreasing trend in ester yield as the catalyst loading increased.

Analysis of the reaction solutions gave a complex yield of reaction products, with esters and phytol as the predominant components of the complex mixture. C_{11}-C_{16}

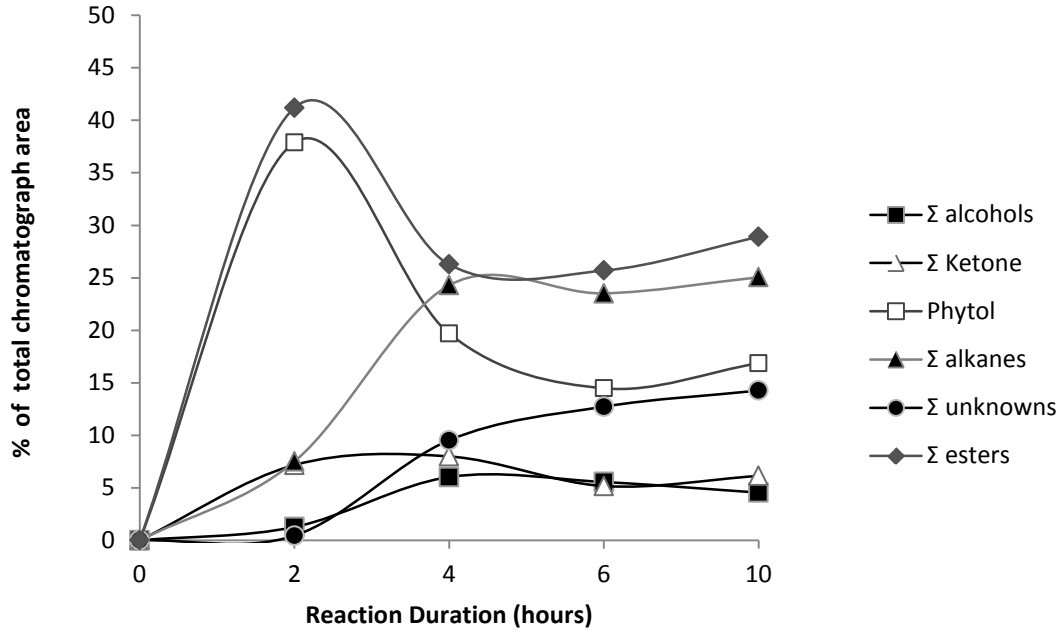

Figure 5.6 Change in reaction products during the course of the reaction.

esters increased throughout the entire reaction duration; however, C_{18} esters (the primary esters observed) decreased significantly between two hours and the subsequent durations. This decrease in C_{18} esters, while other reaction products (including alcohols and ketones) increased, indicates that the esters can undergo further reactivity with the resin over time. Therefore, future experimental research with mixed bed resins must be aware that ester yields can and do change as a function of time in these systems.

6. SUMMARY OF KEY FINDINGS AND PROPOSED FUTURE WORK

6.1 Summary

This research verified that resins containing basic quaternary ammonium functional groups can be used to deacidify feed stocks with high levels of FFA. An increase in feed stock moisture content above 5% total moisture by weight was found to reduce deacidification, while increases in temperature and mixing rate enhanced deacidification. The resins were regenerated using methanol as a resin wash solution. Use of a 1% NaOH in methanol solution was also successfully used to regenerate the resin following deacidification. However, deacidification decreased over successive washes with NaOH present due to saponification. Esters and alcohols were observed in the wash solutions during subsequent analysis.

Basic resins can also be used for transesterification of purified feed stocks (soybean oil with < 1% FFA) in the presence of alcohol. The resulting reaction kinetics of the reaction fit both the ER and LHHW surface models. Further evaluation of the models indicates that when methanol is present in excess the impact of the initial triglyceride concentration in the reactor decreases and the LHHW model reduces to the ER model. When methanol is present in excess, FFA present in the feedstock also increases the rate constant for methanol consumption from 2.08×10^{-7}/sec to 5.39×10^{-4}/sec in the ER model.

The research further demonstrated that the same heterogeneous resin system used for oil deacidification was able to foster in-situ conversion of algal biomass to biodiesel and

other recoverable organics with simultaneous algal extraction and reaction. The algal drying technique had an observable impact of the resulting lipid composition when the algae lipid content was characterized for polar and non-polar lipid content. Due to compositional differences in lipid content, a higher ester yield was observed with air dried algae compared to sun dried for the same reaction conditions and resin. Analysis of the resulting reaction solutions for both algae samples produced a complex yield of reaction products. Esters and phytol were the most predominant reaction products and C_{11}-C_{16} esters increased throughout the entire reaction duration. However, C_{18} esters (the primary esters observed) decreased significantly over the reaction duration of 10 hours. This observed decrease in C_{18} esters occurred as other reaction products were (including alcohols and ketones) increasing, indicating that esters can undergo further reactivity with mixed bed resin over time. Therefore, future experimental work with mixed bed resin systems should be aware that ester yields can and do change as a function of time in these systems.

6.2 Future work

The market for energy fuels for heating and transportation will continue increasing. However, at present the future of biodiesel as an alternative fuel is not promising. Currently, the US biodiesel market is dependent on subsidies the industry is receiving from the government. Under such circumstances, the industry's survival without subsidies will be dependent on finding methods that lead to processing and operations cost savings. This is where research will continue to play an important role.

I am interested in several research topics that I believe will offer promising alternatives within the market and will reduce costs. One area I am interested in is developing continuous lipid separation processes from human and cattle waste based on electrical and mechanical pulsation techniques with simultaneous conversion of the separated lipids into various biofuels. Catalysis of the separated lipids could occur over heterogeneous catalysts operating at temperatures below 50 °C and at atmospheric pressure. I am also interested to learn more about chemical and mechanical methods used to dry biomasses.

Another area I am interested in involves efficient separation and regeneration of heterogeneous catalysts from reaction mixtures. Developing nanomagnetic catalysts with functional covering of quaternary ammonium and sulfonic acid groups is interesting. Use of magnetic catalysts will address separation and regeneration issues currently hampering use of heterogeneous catalysts in full scale systems. Alternatively, novel reactor designs, such as basket type continuous and batch type reactors, may also be used to address the separations issue.

I also believe that in-situ biomass processing with low temperature catalytic pyrolysis supplemented with the use of organic solvents will be a fruitful research area. Development of stable catalysts with custom oxygen bounding functional groups can be used to produce higher energy content pyrolyzed oils. The produced hydrocarbon fraction could then be distilled and used for specific industrial applications such as blending with gasoline. Low temperature catalytic pyrolysis will also use second generation lignocelluloses feed stocks. Finally, standardized on-line laboratory systems

(including instrumentation, sensors and metering devices) are an area of future research interest that could lead to wider commercialization.

REFERENCES

(1) Russbueldt, B. M. E.; Hoelderich, W. F. New sulfonic acid ion-exchange resins for the preesterification of different oils and fats with high content of free fatty acids. *Appl. Catal., A.* **2009,** *362* (1-2), 47-57.

(2) Pasqualino, J. C.; Montané, D.; Salvadó, J. Synergic effects of biodiesel in the biodegradability of fossil-derived fuels. *Biomass Bioenerg.* **2006,** *30* (10), 874-879.

(3) Lin, L.; Cunshan, Z.; Vittayapadung, S.; Xiangqian, S.; Mingdong, D. Opportunities and challenges for biodiesel fuel. *Appl. Energy.* **2011,** *88* (4), 1020-1031.

(4) Saydut, A.; Kafadar, A. B.; Tonbul, Y.; Kaya, C.; Aydin, F.; Hamamci, C. Comparison of the biodiesel quality produced from refined sunflower (Helianthus annuus L) oil and waste cooking oil. *Energy Explor. Exploit.* **2010,** *28* (6), 499-512.

(5) Wang, Y.; Ou, S.; Liu, P.; Zhang, Z. Preparation of biodiesel from waste cooking oil via two-step catalyzed process. *Energy Convers. Manage.* **2007,** *48* (1), 184-188.

(6) Fon Sing, S.; Isdepsky, A.; Borowitzka, M.; Moheimani, N. Production of biofuels from microalgae. *Mitig. Adapt. Strat. Global Change.* Accepted: 25 April 2011. DOI 10.1007/s11027-011-9294-x.

(7) Mondala, A.; Liang, K.; Toghiani, H.; Hernandez, R.; French, T. Biodiesel production by in situ transesterification of municipal primary and secondary sludges. *Bioresour. Technol.* **2009,** *100* (3), 1203-1210.

(8) Predojević, Z. J. The production of biodiesel from waste frying oils: A comparison of different purification steps. *Fuel.* **2008,** *87* (17–18), 3522-3528.

(9) Pinzi, S.; Garcia, I. L.; Lopez-Gimenez, F. J.; Luque de Castro, M. D.; Dorado, G.; Dorado, M. P. The ideal vegetable oil-based biodiesel composition: A review of social, economical and technical implications. *Energy Fuels.* **2009,** *23* (5), 2325-2341.

(10) Berrios, M.; Skelton, R. L. Comparison of purification methods for biodiesel. *Chem. Eng. J.* **2008,** *144* (3), 459-465.

(11) Knothe, G. Analyzing biodiesel: standards and other methods. *J. Am. Oil Chem. Soc.* **2006,** *83* (10), 823-833.

(12) Gerpen, J. V. *Biodiesel Production and Fuel Quality*; University of Idaho: Moscow Idaho, 2005.

(13) U.S. & Canada Biodiesel Plant Map: Existing Plants. http://www.biodieselmagazine.com/plants/listplants/USA/existing (accessed July 13, 2012).

(14) U.S. & Canada Biodiesel Plant Map: Under Construction. http://www.biodieselmagazine.com/plants/listplants/USA/construction (accessed July 13, 2012).

(15) Issariyakul, T.; Kulkarni, M. G.; Dalai, A. K.; Bakhshi, N. N. Production of biodiesel from waste fryer grease using mixed methanol/ethanol system. *Fuel Process. Technol.* **2007,** *88* (5), 429-436.

(16) Özbay, N.; Oktar, N.; Tapan, N. A. Esterification of free fatty acids in waste cooking oils (WCO): Role of ion-exchange resins. *Fuel.* **2008,** *87* (10-11), 1789-1798.

(17) Dufreche, S.; Hernandez, R.; French, T.; Sparks, D.; Zappi, M.; Alley, E. Extraction of lipids from municipal wastewater plant microorganisms for production of biodiesel. *J. Am. Oil Chem. Soc.* **2007,** *84* (2), 181-187.

(18) Kargbo, D. M. Biodiesel production from municipal sewage sludges. *Energy Fuels.* **2010,** *24* (5), 2791-2794.

(19) Chisti, Y. Biodiesel from microalgae. *Biotechnol. Adv.* **2007,** *25* (3), 294-306.

(20) Shibasaki-Kitakawa, N.; Tsuji, T.; Chida, K.; Kubo, M.; Yonemoto, T. Simple continuous production process of biodiesel fuel from oil with high content of free fatty acid using ion-exchange resin catalysts. *Energy Fuels.* **2010,** *24* (6), 3634-3638.

(21) Feng, Y.; He, B.; Cao, Y.; Li, J.; Liu, M.; Yan, F.; Liang, X. Biodiesel production using cation-exchange resin as heterogeneous catalyst. *Bioresour. Technol.* **2010,** *101* (5), 1518-1521.

(22) Canakci, M.; Van Gerpen, J. Biodiesel production via acid catalysis. *Trans. ASAE.* **1999,** *42* (5), 1203-1210.

(23) Mustufa Canakci, J. V. G. Biodiesel Production from oils and fats with high free fatty acids. *Am. Soc. Agric. Eng.* **2001,** *44* (6), 1429–1436.

(24) Fukuda, H.; Kondo, A.; Noda, H. Biodiesel fuel production by transesterification of oils. *J. Biosci. Bioeng.* **2001,** *92* (5), 405-416.

(25) Wang, C. Experimental study on methanol recovery through flashing vaporation in continuous production of biodiesel via supercritical methanol. *Energy Convers. Manage.* **2011,** *52* (2), 1454-1458.

(26) Tan, K. T.; Gui, M. M.; Lee, K. T.; Mohamed, A. R. Supercritical alcohol technology in biodiesel production: A comparative study between methanol and ethanol. *Energy Sources, Part A.* **2011,** *33* (2), 156-163.

(27) Cren, É. C.; Cardozo Filho, L.; Silva, E. A.; Meirelles, A. J. A. Breakthrough curves for oleic acid removal from ethanolic solutions using a strong anion exchange resin. *Sep Purif Technol.* **2009,** *69* (1), 1-6.

(28) Marchetti, J. M.; Miguel, V. U.; Errazu, A. F. Heterogeneous esterification of oil with high amount of free fatty acids. *Fuel.* **2007,** *86* (5–6), 906-910.

(29) Lee, D.-W.; Park, Y.-M.; Lee, K.-Y. Heterogeneous base catalysts for transesterification in biodiesel synthesis. *Catal. Surv. Asia.* **2009,** *13* (2), 63-77.

(30) Feng, Y.; Zhang, A.; Li, J.; He, B. A continuous process for biodiesel production in a fixed bed reactor packed with cation-exchange resin as heterogeneous catalyst. *Bioresour. Technol.* **2011,** *102* (3), 3607-3609.

(31) Shibasaki-Kitakawa, N.; Honda, H.; Kuribayashi, H.; Toda, T.; Fukumura, T.; Yonemoto, T. Biodiesel production using anionic ion-exchange resin as heterogeneous catalyst. *Bioresour. Technol.* **2007,** *98* (2), 416-421.

(32) Jamal, Y.; Boulanger, B. O. Separation of oleic acid from soybean oil using mixed-bed resins. *J. Chem. Eng. Data.* **2010,** *55* (7), 2405-2409.

(33) Ehimen, E. A.; Sun, Z. F.; Carrington, C. G. Variables affecting the in situ transesterification of microalgae lipids. *Fuel.* **2010,** *89* (3), 677-684.

(34) Li, P.; Miao, X.; Li, R.; Zhong, J. In situ biodiesel production from fast-growing and high oil content chlorella pyrenoidosa in rice straw hydrolysate. *J. Biomed. Biotechnol.* **2011,** *2011*.

(35) Di Serio, M.; Tesser, R.; Pengmei, L.; Santacesaria, E. Heterogeneous catalysts for biodiesel production. *Energy Fuels.* **2007,** *22* (1), 207-217.

(36) Balasubramanian, R. K. Heterogeneous catalysis of plant derived oils to biodiesel. Ph.D. Thesis, National University of Singapore, Singapore, 2010.

(37) Kim, M.; Salley, S. O.; Ng, K. Y. S. Transesterification of glycerides using a heterogeneous resin catalyst combined with a homogeneous catalyst. *Energy Fuels.* **2008,** *22* (6), 3594-3599.

(38) de Rezende, S. M.; de Castro Reis, M.; Reid, M. G.; Lúcio Silva Jr, P.; Coutinho, F. M. B.; da Silva San Gil, R. A.; Lachter, E. R. Transesterification of vegetable oils promoted by poly(styrene-divinylbenzene) and poly(divinylbenzene). *Applied Catalysis A: General.* **2008,** *349* (1-2), 198-203.

(39) Li, Y.; Lian, S.; Tong, D.; Song, R.; Yang, W.; Fan, Y.; Qing, R.; Hu, C. One-step production of biodiesel from Nannochloropsis sp. on solid base Mg-Zr catalyst. *Appl. Energy.* **2011,** *In Press, Corrected Proof*.

(40) Dasari, M. A.; Kiatsimkul, P.-P.; Sutterlin, W. R.; Suppes, G. J. Low-pressure hydrogenolysis of glycerol to propylene glycol. *Applied Catalysis A: General.* **2005,** *281* (1–2), 225-231.

(41) Brandin, J.; Hulteberg, C.; Nilsson, A. L. *Bio-Propane from Glycerol for Biogas Addition*; Rapport SGC 198; Lund University: Lund Sweden, 2008.

(42) Gupta, V. P. Glycerine ditertiary butyl ether preparation. US Patent 5,476,971, 1995.

(43) Inbaraj, B. S.; Sulochana, N. Mercury adsorption on a carbon sorbent derived from fruit shell of *Terminalia catappa*. *J. Hazard. Mater.* **2006,** *B133*, 283-290.

(44) DOWEX™ MONOSPHERE™ MR-450 UPW; Form No. 177-01717-402X; The Dow Chemical Company: Midland, MI, 2002.

(45) The Dow Chemical Company. DOWEX™ MONOSPHERE™ MR-450 UPW Mixed Bed Ion Exchange Resin. http://www.dowwaterandprocess.com/products/ix/dx_mn_mr450upw.htm (assessed July 18, 2012).

(46) Cren, E. r. C.; Morelli, A. C.; Sanches, T.; Rodrigues, C. E.; Meirelles, A. J. A. Adsorption isotherms for removal of linoleic acid from ethanolic solutions using the strong anion exchange resin Amberlyst A26 OH. *J. Chem. Eng. Data.* **2010,** *55* (7), 2563-2566.

(47) Cren, É. C.; Meirelles, A. J. A. Adsorption isotherms for oleic acid removal from ethanol + water solutions using the strong anion-exchange resin Amberlyst A26 OH. *J. Chem. Eng. Data.* **2005,** *50* (5), 1529-1534.

(48) Eychenne, V.; Mouloungui, Z. Deacidification of a synthetic oil with an anion exchange resin. *J. Am. Oil Chem. Soc.* **1998,** *75* (10), 1437-1440.

(49) Lotero, E.; Liu, Y.; Lopez, D. E.; Suwannakarn, K.; Bruce, D. A.; Goodwin, J. G. Synthesis of biodiesel via acid catalysis. *Ind. Eng. Chem. Res.* **2005,** *44* (14), 5353-5363.

(50) Liu, Y.; Lotero, E.; Goodwin Jr, J. G.; Lu, C. Transesterification of triacetin using solid brønsted bases. *J. Catal.* **2007,** *246* (2), 428-433.

(51) Dorfiner, K. *Ion Exchangers: Properties and Applications;* Ann Arbor Science: Ann Arbor, MI, 1972.

(52) Isahak, W. N. R. W., M. Ismail, M.A. Yarmo, J.M. Jahim and J. Salimon. Purification of crude glycerol from transesterification RBD palm oil over homogeneous and heterogeneous catalysts for the biolubricant preparation. *J. Appl. Sci.* **2010,** *10* (21), 2590-2595.

(53) Agarwal, M.; Singh, K.; Chaurasia, S. P. Kinetic modeling for biodiesel production by heterogeneous catalysis. *J. Renewable Sustainable Energy.* **2012,** *4* (1), 701-9.

(54) Alkabbashi, A. N.; Md Z. Alam; M.E.S. Mirghani; Al-Fusaiel., A. M. A. Biodiesel production from crude palm oil by transesterification process. *J. Appl. Sci.* **2009,** *9* (17), 3166-3170.

(55) Leung, D. Y. C.; Guo, Y. Transesterification of neat and used frying oil: Optimization for biodiesel production. *Fuel Process. Technol.* **2006,** *87* (10), 883-890.

(56) Kapil, A.; Wilson, K.; Lee, A. F.; Sadhukhan, J. Kinetic modeling studies of heterogeneously catalyzed biodiesel synthesis reactions. *Ind. Eng. Chem. Res.* **2011,** *50* (9), 4818-4830.

(57) Dossin, T. F.; Reyniers, M.-F.; Marin, G. B. Kinetics of heterogeneously MgO-catalyzed transesterification. *Appl. Catal., B.* **2006,** *62* (1–2), 35-45.

(58) Ilgen, O. Reaction kinetics of dolomite catalyzed transesterification of canola oil and methanol. *Fuel Process. Technol.* **2012,** *95*, 62-66.

(59) Veljković, V. B.; Stamenković, O. S.; Todorović, Z. B.; Lazić, M. L.; Skala, D. U. Kinetics of sunflower oil methanolysis catalyzed by calcium oxide. *Fuel.* **2009,** *88* (9), 1554-1562.

(60) Dossin, T. F.; Reyniers, M.-F.; Berger, R. J.; Marin, G. B. Simulation of heterogeneously MgO-catalyzed transesterification for fine-chemical and biodiesel industrial production. *Appl. Catal., B.* **2006,** *67* (1–2), 136-148.

(61) De Filippis, P.; Borgianni, C.; Paolucci, M. Rapeseed oil transesterification catalyzed by sodium phosphates. *Energy Fuels.* **2005,** *19* (6), 2225-2228.

(62) Arzamendi, G.; Campo, I.; Arguiñarena, E.; Sánchez, M.; Montes, M.; Gandía, L. M. Synthesis of biodiesel from sunflower oil with silica-supported NaOH catalysts. *J. Chem. Technol. Biotechnol.* **2008,** *83* (6), 862-870.

(63) Cantrell, D. G.; Gillie, L. J.; Lee, A. F.; Wilson, K. Structure-reactivity correlations in MgAl hydrotalcite catalysts for biodiesel synthesis. *Appl. Catal., A.* **2005,** *287* (2), 183-190.

(64) Marchetti, J. M.; Errazu, A. F. Biodiesel production from acid oils and ethanol using a solid basic resin as catalyst. *Biomass Bioenergy.* **2010,** *34* (3), 272-277.

(65) Munari, F.; Cavagnino, D.; Cadoppi, A. *Determination of Total FAME and Linolenic Acid Methyl Ester in Pure Biodiesel (B100) by GC in Compliance with*

EN 14103; Application Note: 10212; Thermo Fisher Scientific: Milan, Italy, 2007.

(66) Ralf, W.; Bähren, A. *Application Book Volume 4: Biodiesel Quality Control*; Shimadzu Europa Gmbh: Duisburg, Germany, 2008.

(67) Converti, A.; Casazza, A. A.; Ortiz, E. Y.; Perego, P.; Del Borghi, M. Effect of temperature and nitrogen concentration on the growth and lipid content of Nannochloropsis oculata and Chlorella vulgaris for biodiesel production. *Chemical Engineering and Processing: Process Intensification.* **2009,** *48* (6), 1146-1151.

(68) Widjaja, A.; Chien, C.-C.; Ju, Y.-H. Study of increasing lipid production from fresh water microalgae Chlorella vulgaris. *J. Taiwan Inst. Chem. Eng.* **2009,** *40* (1), 13-20.

(69) Beal, C. M.; Hebner, R. E.; Romanovicz, D.; Mayer, C. C.; Connelly, R. Progression of lipid profile and cell structure in a research-scale production pathway for algal biocrude. *Renewable Energy.* **2013,** *50* (0), 86-93.

(70) Dyn´ska-Kukulska, K.; Ciesielski, W. Methods of extraction and thin-layer chromatography determination of phospholipids in biological samples. *Rev. Anal. Chem.* **2012,** *31* (1), 43-56.

(71) Danielewicz, M. A.; Anderson, L. A.; Franz, A. K. Triacylglycerol profiling of marine microalgae by mass spectrometry. *J. Lipid Res.* **2011,** *52* (11), 2101-2108.

(72) Danielewicz, M. A.; Anderson, L. A.; Franz, A. K. Supplementary Information: Triacylglycerol Profiling of Marine Microalgae by Mass Spectrometry.

http://www.jlr.org/content/suppl/2011/08/11/jlr.D018408.DC1/jlr.D018408-1.pdf (accessed July 2, 2012).

(73) Byrdwell, W. C. Taking Lipid Analysis into the 21st Century. http://www.byrdwell.com/Triacylglycerols (accessed July 17, 2012).

(74) Li, H.; Pordesimo, L.; Weiss, J. High intensity ultrasound-assisted extraction of oil from soybeans. *Food Res. Int.* **2004,** *37* (7), 731-738.

(75) Perneta, F.; Tremblayb, R. Effect of ultrasonication and grinding on the determination of lipid class content of microalgae harvested on filters. *Lipids.* **2003,** *38* (11), 1191-95.

(76) Ryckebosch, E.; Muylaert, K.; Foubert, I. Optimization of an analytical procedure for extraction of lipids from microalgae. *J. Am. Oil Chem. Soc.* **2012,** *89* (2), 189-198.

(77) Chung, E.-A.; Cho, C.-W.; Ahn, K. H. Direct conversion of carboxylic esters into ketones using organoaluminum complexes. *J. Org. Chem.* **1998,** *63* (22), 7590-7591.

(78) Christie, W. W. Waxes: Structure, Composition, Occurrence and Analysis. http://lipidlibrary.aocs.org/lipids/waxes/index.htm (accessed June 21, 2012).

APPENDIX A

ER SURFACE REACTION MODEL DERIVATION

Based upon the assumptions provided in Section 4.2.2, the following series of equations can be derived for ER surface reaction model solution. The stepwise reactions in the ER model derivation include:

Step 1: $$\mathrm{MeOH} + * \underset{k\_1}{\overset{k1}{\rightleftarrows}} \mathrm{MeOH}^* \quad (1)$$

Step 2: $$\mathrm{T} + \mathrm{MeOH}^* \underset{k\_2}{\overset{k2}{\rightleftarrows}} \mathrm{E} + \mathrm{D}^* \quad (2)$$

Step 3: $$\mathrm{D} + \mathrm{MeOH}^* \underset{k\_3}{\overset{k3}{\rightleftarrows}} \mathrm{E} + \mathrm{M}^* \quad (3)$$

Step 4: $$\mathrm{M} + \mathrm{MeOH}^* \underset{k\_4}{\overset{k4}{\rightleftarrows}} \mathrm{E} + \mathrm{G}^* \quad (4)$$

Step 5: $$\mathrm{D} + * \underset{k\_5}{\overset{k5}{\rightleftarrows}} \mathrm{D}^* \quad (5)$$

Step 6: $$\mathrm{M} + * \underset{k\_6}{\overset{k6}{\rightleftarrows}} \mathrm{M}^* \quad (6)$$

Step 7: $$\mathrm{G} + * \underset{k\_7}{\overset{k7}{\rightleftarrows}} \mathrm{G}^* \quad (7)$$

where: MeOH = methanol; T = triglyceride; E = methyl ester; G = glycerol; * = resin surface site; and MeOH*, T*, E*, D*, M* and G* are bounded resin surface sites; k_n=forward reaction; $k\text{-}_{n=}$ backward reaction, n = reaction step

Note: $K_{Adsorption} = \frac{k_{forward}}{k_{backward}}$ and $K_{Desorption} = \frac{k_{backward}}{k_{forward}}$

Therefore, the rate equations for the adsorption of methanol and the surface reaction of adsorbed MeOH with T, D, M, and G can be written as follows:

Methanol adsorption as rate limiting step

$$r_1 = k_1[MeOH][*] - k_{-1}[MeOH^*] \quad (8)$$

$$K_1 = \frac{k_1}{k_{-1}}$$

$$r_1 = k_1\left([MeOH][*] - \frac{1}{K_1}[MeOH^*]\right) \quad (8a)$$

Because MeOH adsorption is the rate limiting step, k_2 through k_7 will be much larger than k_1. Therefore, $\frac{r_2}{k_2}$, $\frac{r_3}{k_3}$, $\frac{r_4}{k_4}$, $\frac{r_5}{k_5}$, $\frac{r_6}{k_6}$ and $\frac{r_7}{k_7}$ in the following series of equations are assumed to be very small (almost zero).

Rate of triglycerides surface reaction

$$r_2 = k_2[MeOH^*][T] - k_{-2}[D^*][E] \quad (9)$$

$$K_2 = \frac{k_2}{k_{-2}}$$

$$\frac{r_2}{k_2} \cong 0 = \left([MeOH^*][T] - \frac{1}{K_2}[D^*][E]\right) \quad (9a)$$

Rate of diglycerides surface reaction

$$r_3 = k_3[MeOH^*][D] - k_{-3}[M^*][E] \quad (10)$$

$$K_3 = \frac{k_3}{k_{-3}}$$

$$\frac{r_3}{k_3} \cong 0 = \left([MeOH^*][D] - \frac{1}{K_3}[M^*][E]\right) \quad (10a)$$

Rate of monoglycerides surface reaction

$$r_4 = k_4[MeOH^*][M] - k_{-4}[G^*][E] \quad (11)$$

$$K_4 = \frac{k_4}{k_{-4}}$$

$$\frac{r_4}{k_4} \cong 0 = \left([MeOH^*][D] - \frac{1}{K_4}[M^*][E]\right) \quad (11a)$$

Rate of diglycerides desorption:

$$r_5 = k_5[D][*] - k_{-5}[D^*] \quad (12)$$

$$K_5 = \frac{k_5}{k_{-5}}$$

$$\frac{r_5}{k_5} \cong 0 = \left([D][*] - \frac{1}{K_5}[D^*]\right)$$

$$[D*] = K_5[D][*] \quad (12a)$$

Rate of monoglycerides desorption:

$$r_6 = k_6[M][*] - k_{-6}[M^*] \quad (13)$$

$$K_6 = \frac{k_6}{k_{-6}}$$

$$\frac{r_6}{k_6} \cong 0 = \left([M][*] - \frac{1}{K_6}[M^*]\right)$$

$$[M*] = K_6[M][*] \quad (13a)$$

Rate of glycerol desorption:

$$r_7 = k_7[G][*] - k_{-7}[G^*] \quad (14)$$

$$K_7 = \frac{k_7}{k_{-7}}$$

$$\frac{r_7}{k_7} \cong 0 = \left([G][*] - \frac{1}{K_7}[G^*]\right)$$

$$[G*] = K_7[G][*] \quad (14a)$$

Solving for [MeOH*] in equations (9a-14a)

$$[MeOH^*] = \frac{1}{K_4}\frac{[G^*][E]}{[M]} = \frac{1}{K_4}\frac{K_7[G][E][*]}{[M]} \quad (15)$$

$$[MeOH^*] = \frac{1}{K_3}\frac{[M^*][E]}{[D]} = \frac{1}{K_3}\frac{K_6[M][E][*]}{[D]} \quad (16)$$

$$[MeOH^*] = \frac{1}{K_2}\frac{[D^*][E]}{[T]} = \frac{1}{K_2}\frac{K_5[D][E][*]}{[T]} \quad (17)$$

Therefore, $$[MeOH^*] = \left(\frac{1}{K_4}\frac{K_7[G]}{[M]} = \frac{1}{K_3}\frac{K_6[M]}{[D]} = \frac{1}{K_2}\frac{K_5[D]}{[T]}\right)[E][*] \quad (18)$$

The equation that represents the overall mass balance on the surface sites is:

$$S_T = [*] + [\mathrm{MeOH}^*] + [\mathrm{D}^*] + [\mathrm{M}^*] + [\mathrm{G}^*] \quad (19)$$

where S_T is the total binding sites on the surface.

Considering $[\mathrm{MeOH}^*] = \frac{1}{K_2}\frac{K_5[D][E][*]}{[T]}$ (20)

and substituting [MeOH*] into the site balance equation

$$S_T = \left([*] + \left(\frac{1}{K_2}\frac{K_5[D][E][*]}{[T]}\right) + K_5[D][*] + K_6[M][*] + K_7[G][*]\right) \quad (21)$$

$$[*] = \frac{S_T}{\left([1] + \left(\frac{1}{K_2}\frac{K_5[D][E]}{[T]}\right) + K_5[D] + K_6[M] + K_7[G]\right)} \quad (22)$$

Rate of methanol adsorption from equation 8a

$$r_1 = k_1\left([\mathrm{MeOH}][*] - \frac{1}{K_1}[\mathrm{MeOH}^*]\right)$$

Substituting in the value of $[\mathrm{MeOH}^*]$ from equation 20

$$r_1 = k_1\left([\mathrm{MeOH}][*] - \frac{1}{K_1}\left(\frac{1}{K_2}\frac{K_5[D][E][*]}{[T]}\right)\right)$$

$$r_1 = k_1\left([\mathrm{MeOH}] - \frac{1}{K_1}\left(\frac{1}{K_2}\frac{K_5[D][E]}{[T]}\right)\right)[*]$$

Substituting in the value of [*] from equation 22

$$r_1 = \frac{k_1 S_T\left([MeOH] - \frac{1}{K_1}\left(\frac{1\ K_5[D][E]}{K_2\ \ [T]}\right)\right)}{\left([1] + \left(\frac{1\ K_5[D][E]}{K_2\ \ [T]}\right) + K_5[D] + K_6[M] + K_7[G]\right)} \quad (23)$$

Because the model assumes that methanol adsorption is the rate limiting step, neglecting the presence of intermediates formed during the reaction and combining $k_1 S_T$ into k reduces the model to the following final form shown in equation 24.

Rate of methanol consumption

$$r_1 = \frac{d[MeOH]}{dt} = -\frac{k([MeOH])}{([1] + K_7[G])} \quad (24)$$

For the case of high FA content in soybean oil, an additional term for FFA adsorbed at the resin surface only is added to the model in the following form.

Rate of FFA adsorption:

$$r_8 = k_8[FFA][*] - k_{-8}[FFA^*] \quad (25)$$

$$K_8 = \frac{k_8}{k_{-8}}$$

$$\frac{r_8}{k_8} \cong 0 = \left([FFA][*] - \frac{1}{K_8}[FFA^*]\right)$$

$$[FFA\,*] = K_8[FFA][*] \quad (25a)$$

The site balance from equation (21) with this additional term becomes

$$S_T = \left([*] + \left(\frac{1}{K_2}\frac{K_5[D][E]\,[*]}{[T]}\right) + K_5[D][*] + K_6[M][*] + K_7[G][*] + K_8[FFA][*]\right) \quad (26)$$

which represents the addition of one extra term to the derivation of the methanol adsorption:

$$r_1 = -\frac{k_{MeOH}S_T\left([MeOH] - \frac{1}{K_{eq}}\left(\frac{1}{K_2}\frac{K_5[D][E]}{[T]}\right)\right)}{\left([1] + \left(\frac{1}{K_2}\frac{K_5[D][E]}{[T]}\right) + K_5[D] + K_6[M] + K_7[G] + K_8[FFA]\right)} \quad (27)$$

Therefore, equation 28 represents the final derived form of the ER model with FFA present when k_1S_T is combined into k and all assumptions are considered:

$$r_1 = \frac{d[MeOH]}{dt} = -\frac{k([MeOH])}{([1] + K_7[G] + K_8[FFA])} \quad (28)$$

APPENDIX B

LHHW SURFACE REACTION MODEL DERIVATION

Based upon the assumptions provided in Section 4.2.2, the following series of equations can be derived for the LHHW surface reaction model solution. The stepwise reactions in LHHW model derivation include:

Step 1: $$MeOH + * \underset{k-1}{\overset{k1}{\rightleftarrows}} MeOH^* \quad (1)$$

Step 2: $$T + * \underset{k-2}{\overset{k2}{\rightleftarrows}} T^* \quad (2)$$

Step 3: $$T^* + MeOH^* \underset{k-3}{\overset{k3}{\rightleftarrows}} E^* + D^* \quad (3)$$

Step 4: $$D^* + MeOH^* \underset{k-4}{\overset{k4}{\rightleftarrows}} E^* + M^* \quad (4)$$

Step 5: $$M^* + MeOH^* \underset{k-5}{\overset{k5}{\rightleftarrows}} E^* + G^* \quad (5)$$

Step 6: $$E + * \underset{k-6}{\overset{k6}{\rightleftarrows}} E^* \quad (6)$$

Step 7: $$D + * \underset{k-7}{\overset{k7}{\rightleftarrows}} D^* \quad (7)$$

Step 8: $$M + * \underset{k-8}{\overset{k8}{\rightleftarrows}} M^* \quad (8)$$

Step 9: $$G + * \underset{k-9}{\overset{k9}{\rightleftarrows}} G^* \quad (9)$$

where: MeOH = methanol; T = triglyceride; E = methyl ester; G = glycerol; * = resin surface site; and MeOH*, T*, E*, D*, M*, and G* are bounded resin surface sites; k_n=forward reaction; k_{-n}= backward reaction, n = reaction step

Note: $K_{Adsorption} = \frac{k_{forward}}{k_{backward}}$ and $K_{Desorption} = \frac{k_{backward}}{k_{forward}}$

Therefore, the rate equations for the adsorption of methanol and the surface reaction of adsorbed MeOH with T, D, M, and G can be written as follows:

Methanol adsorption as rate limiting step

$$r_1 = k_1[MeOH][*] - k_{-1}[MeOH^*] \quad (10)$$

$$K_1 = \frac{k_1}{k_{-1}}$$

$$r_1 = k_1\left([MeOH][*] - \frac{1}{K_1}[MeOH^*]\right) \quad (10a)$$

Because MeOH adsorption is the rate limiting step, k_2 through k_9 will be much larger than k_1. Therefore, $\frac{r_2}{k_2}$, $\frac{r_3}{k_3}$, $\frac{r_4}{k_4}$, $\frac{r_5}{k_5}$, $\frac{r_6}{k_6}$, $\frac{r_7}{k_7}$, $\frac{r_8}{k_8}$, and $\frac{r_9}{k_9}$ in the following series of equations are assumed to be very small (almost zero).

Rate of triglycerides adsorption:

$$r_2 = k_2[T][*] - k_{-2}[T^*] \quad (11)$$

$$K_2 = \frac{k_2}{k_{-2}}$$

$$\frac{r_2}{k_2} \cong 0 = \left([T][*] - \frac{1}{K_2}[T^*]\right) \quad (11a)$$

Rate of surface reaction of bound triglyceride with bound methanol

$$r_3 = k_3[MeOH^*][T^*] - k_{-3}[D^*][E^*] \quad (12)$$

$$K_3 = \frac{k_3}{k_{-3}}$$

$$\frac{r_3}{k_3} \cong 0 = \left([MeOH^*][T^*] - \frac{1}{K_3}[D^*][E^*]\right) \quad (12a)$$

Rate of diglycerides surface reaction

$$r_4 = k_4[MeOH^*][D^*] - k_{-4}[M^*][E^*] \quad (13)$$

$$K_4 = \frac{k_4}{k_{-4}}$$

$$\frac{r_4}{k_4} \cong 0 = \left([MeOH^*][D^*] - \frac{1}{K_4}[M^*][E^*]\right) \quad (13a)$$

Rate of monoglyceride surface reaction

$$r_5 = k_5[MeOH^*][M^*] - k_{-5}[G^*][E^*] \quad (14)$$

$$K_5 = \frac{k_5}{k_{-5}}$$

$$\frac{r_5}{k_5} \cong 0 = \left([MeOH^*][M^*] - \frac{1}{K_5}[G^*][E^*]\right) \quad (14a)$$

Rate of methyl ester desorption

$$r_6 = k_6[E][*] - k_{-6}[E^*] \quad (15)$$

$$K_6 = \frac{k_6}{k_{-6}}$$

$$\frac{r_6}{k_6} \cong 0 = \left([E][*] - \frac{1}{K_6}[E^*]\right)$$

$$[E*] = K_6[E][*] \quad (15a)$$

Rate of diglycerides desorption

$$r_7 = k_7[D][*] - k_{-7}[D^*] \quad (16)$$

$$K_7 = \frac{k_7}{k_{-7}}$$

$$\frac{r_7}{k_7} \cong 0 = \left([D][*] - \frac{1}{K_7}[D^*]\right)$$

$$[D*] = K_7[D][*] \quad (16a)$$

Rate of monoglycerides desorption

$$r_8 = k_8[M][*] - k_{-8}[M^*] \quad (17)$$

$$K_8 = \frac{k_8}{k_{-8}}$$

$$\frac{r_8}{k_8} \cong 0 = \left([M][*] - \frac{1}{K_8}[M^*]\right)$$

$$[M*] = K_8[M][*] \quad (17a)$$

Rate of glycerol desorption

$$r_9 = k_9[G][*] - k_{-9}[G^*] \quad (18)$$

$$K_9 = \frac{k_9}{k_{-9}}$$

$$\frac{r_9}{k_9} \cong 0 = \left([G][*] - \frac{1}{K_9}[G^*]\right)$$

$$[G*] = K_7[G][*] \tag{18a}$$

Solving for [MeOH*] in equations (11a-18a)

$$[MeOH^*] = \frac{K_9K_6[G][E][*]}{K_5K_8[M]} = \frac{K_9K_6[G][E][*]}{K_5K_8[M]} \tag{19}$$

$$[MeOH^*] = \frac{K_6K_8[M][E][*]}{K_4K_7[D]} = \frac{K_6K_8[M][E][*]}{K_4K_7[D]} \tag{20}$$

$$[MeOH^*] = \frac{K_6K_7[D][E][*]}{K_3K_2[T]} = \frac{K_6K_7[D][E][*]}{K_3K_2[T]} \tag{21}$$

Therefore $[MeOH^*] = \left(\frac{K_9K_6[G]}{K_5K_8[M]} = \frac{K_6K_8[M]}{K_4K_7[D]} = \frac{K_6K_7[D]}{K_3K_2[T]}\right)[E][*]$

The equation that represents the overall mass balance on the surface sites is:

$$S_T = [*] + [MeOH^*] + [T^*] + [E^*] + [D^*] + [M^*] + [G^*] \tag{22}$$

where S_T is the total binding sites on the surface.

Considering $[MeOH^*] = \frac{K_6K_7[D][E][*]}{K_3K_2[T]}$ (23)

and substituting [MeOH*] into the site balance equation

$$S_T = \left([*] + \left(\frac{K_6K_7[D][E][*]}{K_3K_2[T]}\right) + k_2[T][*] + k_6[E][*] + k_7[D][*] + k_8[M][*] + k_9[G][*]\right) \tag{24}$$

$$[*] = \frac{S_T}{\left([1] + \left(\frac{K_6K_7[D][E]}{K_3K_2[T]}\right) + k_2[T] + k_6[E] + k_7[D] + k_8[M] + k_9[G]\right)} \tag{25}$$

Rate of methanol adsorption from equation 10a is

$$r_1 = k_1\left([MeOH][*] - \frac{1}{K_1}[MeOH^*]\right)$$

Substituting in the value of $[MeOH^*]$ from equation 23

$$r_1 = k_1\left([MeOH][*] - \frac{1}{K_1}\left(\frac{K_6K_7[D][E][*]}{K_3K_2[T]}\right)\right)$$

$$r_1 = k_1\left([MeOH] - \frac{1}{K_1}\left(\frac{K_6K_7[D][E]}{K_3K_2[T]}\right)\right)[*]$$

Substituting in the value of [*] from equation 25

$$r_1 = \frac{k_1S_T\left([MeOH] - \frac{1}{K_1}\left(\frac{K_6K_7[D][E]}{K_3K_2[T]}\right)\right)}{\left([1] + \left(\frac{K_6K_7[D][E]}{K_3K_2[T]}\right) + K_2[T] + K_6[E] + K_7[D] + K_8[M] + K_9[G]\right)} \quad (26)$$

Because the model assumes that methanol adsorption is the rate limiting step, neglecting the presence of intermediates formed during the reaction and combining k_1S_T into k reduces the model to the following final form shown in equation 27.

$$r_1 = \frac{d[MeOH]}{dt} = -\frac{k([MeOH])}{([1] + K_2[T] + K_6[E] + K_9[G])} \quad (27)$$

For the case of high FFA content in soybean oil, an additional term for FFA adsorbed at the resin surface only is added to the model in the following form.

Rate of FFA adsorption:

$$r_{10} = k_{10}[FFA][*] - k_{-10}[FFA^*] \tag{28}$$

$$K_{10} = \frac{k_{10}}{k_{-10}}$$

$$\frac{r_{10}}{k_{10}} \cong 0 = \left([FFA][*] - \frac{1}{K_{10}}[FFA^*]\right)$$

$$[FFA\,*] = K_{10}[FFA][*] \tag{28a}$$

The site balance from equation (24) with this additional term becomes

$$S_T = \begin{pmatrix} [*] + \left(\frac{K_6K_7[D][E][*]}{K_3K_2[T]}\right) + K_2[T][*] + K_6[E][*] + K_7[D][*] + K_8[M][*] \\ +K_9[G][*] + K_{10}[FFA][*] \end{pmatrix} \tag{29}$$

Rearranging eq (29)

$$[*] = \frac{S_T}{\left([1] + \left(\frac{K_6K_7[D][E]}{K_3K_2[T]}\right) + K_2[T] + K_6[E] + K_7[D] + K_8[M] + K_9[G] + K_{10}[FFA]\right)} \tag{30}$$

which represents the addition of one extra term to the derivation of the methanol adsorption:

$$r_1 = -\frac{k_1S_T\left([MeOH] - \frac{1}{K_{eq}}\left(\frac{K_6K_7[D][E]}{K_3K_2[T]}\right)\right)}{\left([1] + \left(\frac{K_6K_7[D][E]}{K_3K_2[T]}\right) + K_2[T] + K_6[E] + k_7[D] + K_8[M] + K_9[G] + K_{10}[FFA]\right)} \tag{31}$$

Therefore, equation 32 represents the final derived form of the LHHW model with FFA present when k_1S_T is combined into k and all assumptions are considered:

$$r_1 = \frac{d[MeOH]}{dt} = -\frac{k([MeOH])}{([1]+K_2[T]+K_6[E]+K_9[G]+K_{10}[FFA])} \quad (32)$$